JOURNAL OF PROTEOMICS 94 (2013) 240–261

Available online at www.sciencedirect.com

ScienceDirect

www.elsevier.com/locate/jprot

Mono-dimensional blue native-PAGE and bi-dimensional blue native/urea-PAGE or/SDS-PAGE combined with nLC–ESI-LIT-MS/MS unveil membrane protein heteromeric and homomeric complexes in *Streptococcus thermophilus*

Anna Maria Salzano[a], *Gianfranco Novi*[a], *Stefania Arioli*[b], *Silvia Corona*[c], *Diego Mora*[b], *Andrea Scaloni*[a,*]

[a]*Proteomics and Mass Spectrometry Laboratory, ISPAAM, National Research Council, 80147 Naples, Italy*
[b]*Department of Food Science and Microbiology, University of Milan, 20133 Milan, Italy*
[c]*IRCCS Policlinico San Matteo, 27100 Pavia, Italy*

ARTICLE INFO

Article history:
Received 11 June 2013
Accepted 14 September 2013

Keywords:
Streptococcus thermophilus
Lactic acid bacterium
Protein complexes
Blue native/urea-PAGE
Blue native/SDS-PAGE
Exopolysaccharide

ABSTRACT

Protein interactions are essential elements for the biological machineries underlying biochemical and physiological mechanisms indispensable for microorganism life. By using mono-dimensional blue native polyacrylamide gel electrophoresis (1D-BN-PAGE), two-dimensional blue native/urea-PAGE (2D-BN/urea-PAGE) and two-dimensional blue native/SDS-PAGE (2D-BN/SDS-PAGE), membrane protein complexes of *Streptococcus thermophilus* were resolved and visualized. Protein complex and oligomer constituents were then identified by nLC–ESI-LIT-MS/MS. In total, 65 heteromeric and 30 homomeric complexes were observed, which were then associated with 110 non-redundant bacterial proteins. Protein machineries involved in polysaccharide biosynthesis, molecular uptake, energy metabolism, cell division, protein secretion, folding and chaperone activities were highly represented in electrophoretic profiles; a number of homomeric moonlighting proteins were also identified. Information on hypothetical proteins was also derived. Parallel genome sequencing unveiled that the genes coding for the enzymes involved in exopolysaccharide biosynthesis derive from two separate clusters, generally showing high variability between bacterial strains, which contribute to a unique, synchronized and active synthetic module. The approach reported here paves the way for a further functional characterization of these protein complexes and will facilitate future studies on their assembly and composition during various growth conditions and in different mutant backgrounds, with important consequences for biotechnological applications of this bacterium in dairy productions.

Abbreviations: 1D-BN-PAGE, mono-dimensional blue native polyacrylamide gel electrophoresis; 2D-BN/SDS-PAGE, two-dimensional blue native/SDS-PAGE; 2D-BN/urea-PAGE, two-dimensional blue native/urea-PAGE; nLC–ESI-LIT-MS/MS, nano-liquid chromatography coupled with electrospray ionization-linear ion trap tandem mass spectrometry.

* *Corresponding author at:* Proteomics & Mass Spectrometry Laboratory, ISPAAM, National Research Council, via Argine 1085, Naples, I-80147, Italy. Tel.: +39 081 5966006; fax: +39 081 5965291.
E-mail address: andrea.scaloni@ispaam.cnr.it (A. Scaloni).

http://dx.doi.org/10.1016/j.jprot.2013.09.007

Biological significance
Combined proteomic procedures have been applied to the characterization of heteromultimeric and homomeric protein complexes from the membrane fraction of *S. thermophilus*. Protein machineries involved in polysaccharide biosynthesis, molecular uptake, energy metabolism, cell division, protein secretion, folding and chaperone activities were identified; information on hypothetical and moonlighting proteins were also derived. This study is original in the lactic bacteria context and may be considered as preliminary to a deeper functional characterization of the corresponding protein complexes. Due to the large use of *S. thermophilus* as a starter for dairy productions, the data reported here may facilitate future investigations on protein complex assembly and composition under different experimental conditions or for bacterial strains having specific biotechnological applications.

1. Introduction

Streptococcus thermophilus is of major importance for the food industry since it is widely used for the manufacture of dairy products; in this context, it is considered as the second most important industrial dairy starter after *Lactococcus lactis* [1,2]. Together with symbiotic *Lactobacillus delbrueckii* subsp. *bulgaricus* or *Lactobacillus helveticus*, this Gram-positive (G+) lactic acid bacterium is generally used for the production at relatively high process temperatures of yogurt and so-called *hard cooked* cheeses (e.g., emmenthal, grana) [1,3]. In combination with other lactobacilli, it is also utilized for the manufacture of mozzarella and cheddar cheeses [1].

S. thermophilus is closely related to *L. lactis* but it is even more strictly related to streptococcal pathogenic species, including *Streptococcus pyogenes*, *Streptococcus agalactiae*, *Streptococcus pneumoniae*, *Streptococcus mutans*, *Streptococcus suis* and *Streptococcus equi*, which cause different lethal infection diseases or tooth decay [4,5]. Nevertheless, *S. thermophilus* is generally recognized as a safe bacterium and a multitude of live microorganism cells are ingested annually by humans. The complete genome sequence of various *S. thermophilus* strains (LMG18311, CNRZ1066, LMD9, JIM8232, ND03 and MNZLW002) was made publicly available (http://www.ncbi.nlm.nih.gov/genome/genomes/420) [6–11]. Its comparison with the genome of streptococcal pathogens highlighted the similitude of this lactic acid bacterium to pathogenic species [6–8], but also revealed that the most significant determinants for pathogenicity are either lacking or present as pseudogenes, except they code essential cellular functions. Comparative genomics also revealed that evolution has shaped the *S. thermophilus* genome mainly through loss-of-function events, even if lateral gene transfer played an important role [12], disclosing that this bacterium has followed an evolutionary path divergent to that of streptococcal pathogens as result to its adaptation to a specific and well-defined ecological niche, i.e. milk.

To investigate global gene expression changes in *S. thermophilus* during exponential and stationary phases or following adaptation to various environmental stresses, we previously characterized changes of the corresponding cytosolic and/or membrane proteomic repertoires by gel-based and shotgun approaches [13–15]. Global characterization of multi-protein complexes is also an important step to provide an integrative view of multipart polypeptide machineries that are essential for bacterial biological functions and physiology. Recent advancements in high throughput technologies have allowed a direct description of protein–protein interactions; thus, two-hybrid assay [16–23], protein chip [24–26] or co-purification [27–29] procedures have been widely used to characterize bacterial protein–protein interaction networks. Recent considerations on restricted accuracy of deriving results and its labor-intensive nature have limited the application of the first two approaches to the production of large scale protein–protein interaction datasets [30,31]. Thus, two functional proteomic technologies based on direct MS identification of resolved protein components have been preferentially used for systematic analysis of co-purified hetero-multimeric and/or homomeric complexes following their affinity capture by tagged-protein baits [28] or their direct resolution by 1D-BN-PAGE and 2D-BN/SDS-PAGE [29]. In both cases, protein complex purification has to be performed under native conditions to prevent molecular dissociation. Protein complex affinity capture by tagged-protein baits allowed the characterization of a number of polypeptide machineries, as in the case of *Escherichia coli* [32–35], *Mycoplasma pneumoniae* [36], *Staphylococcus aureus* [37], *Rhodopseudomonas palustris* and *Shewanella oneidensis* [38], generating large bacterial protein interaction networks. On the other hand, 1D-BN-PAGE and 2D-BN/SDS-PAGE have found a widespread application for the analysis of bacterial complexomes [29,39,40]. Also in this case, a non-denaturing environment must be kept throughout the first dimension BN-PAGE analysis. It comprises the use of: i) neutral pH-low salt concentration buffers, no reducing/denaturing agents, manipulation at low-temperatures and mild zwitterionic detergents for sample preparation; ii) anionic Coomassie Brilliant Blue G-250 dye and Bis–Tris/imidazole during electrophoresis to impose a net negative charge on protein surfaces, thus facilitating protein complex migration, hampering solute aggregation and stabilizing native gel pH value, respectively. Each multi-protein complex may be then denatured in a second dimension electrophoresis (SDS-PAGE), and the protein alignment within the gel allows the MS-based identification of interactive proteins. Alternatively, each protein complex band from 1D-BN-PAGE can be directly analyzed for its constituents by nLC–ESI-MS/MS [41]. Both approaches were used for high-throughput characterization of: i) membrane protein complexes from *Neisseria meningitides* [42], *Rhodobacter sphaeroides* [43], *Francisella tularensis* [44], *Clostridium thermocellum* [45], *Mycobacterium bovis* [46] and *Enterococcus faecalis* [47];

ii) cytoplasmic protein complexes from *Streptomyces coelicolor* [48] and *Pseudomonas* sp. [49]; iii) membrane and cytoplasmic protein complexes from *Helicobacter pylori* [50,51], *E. coli* [52,53], *Chlorobium tepidum* [54,55] and *Methanothermobacter therautotrophicus* [56]. Results from tagged-protein- and BN-PAGE-based experiments allowed compiling various microbial protein interaction database, such as eNet, MPIDB, STRING, IntAct, DIP, BIOGRID and others [57–61], which now can be searched simultaneously by using the dedicated service PSICQUIC interface [62].

In this study, we report on the combined use of 1D-BN-PAGE, 2D-BN/urea-PAGE, 2D-BN/SDS-PAGE, and nLC–ESI-LIT-MS/MS for the characterization of membrane complexes from *S. thermophilus*. A number of molecular machineries, as obtained from the extraction of bacterial membranes with 0.5% *n*-dodecyl-β-D-maltoside (βDDM), were characterized, describing the heteromultimeric or homomeric nature of the corresponding protein complexes and discussing their functional properties with respect to organism physiology.

2. Materials and methods

2.1. Bacterial growth

S. thermophilus strain DSM20617 was grown in M17 medium supplemented with 2% lactose, at 37 °C, without shaking [15]. Cells were monitored by measuring the absorbance at 600 nm, collected in their early exponential phase (pH 5.6) and then washed with sterile 20 mM Tris–HCl, pH 7.4, at 4 °C. Bacterial cells were harvested by centrifugation at 14,000 ×*g*, at 4 °C, and then washed twice in PBS, pH 7.4.

2.2. Protein sample preparation

A biomass corresponding to 5 g of bacterial cells (wet weight) was suspended in extraction buffer (750 mM ε-amino caproic acid, 1 mM PMSF, 50 mM Tris–HCl, pH 7.0) and sonicated in ice with a Labsonic U sonicator, repeating duty cycles of 0.5 s for 60 s, for 5 times, with 15 s intervals. Unbroken cells and cell debris were removed from resulting suspension by centrifugation at 10,000 ×*g*, for 15 min, at 4 °C. DNase I (100 μg/mL final concentration) was added to the supernatant; the sample was kept at 25 °C, for 1 h, and then centrifuged at 100,000 ×*g*, for 30 min, at 4 °C. Membrane pellet was washed once in extraction buffer, at 4 °C, and twice in 0.33 M sorbitol, 1 mM PMSF, 50 mM Bis–Tris–HCl, pH 7.0, at 4 °C. Finally, membrane pellet was resuspended in resuspension buffer (20% v/v glycerol, 1 mM PMSF, 25 mM Bis–Tris–HCl, pH 7.0) at 4 °C, and quantified using the DC protein assay (Bio-Rad Laboratories, Hercules, CA). Under continuous mixing, equal volumes of sample suspension and resuspension buffer containing 1% βDDM (Sigma-Aldrich, St. Louis, MO) were mixed. Solubilization of membrane protein complexes was allowed to occur on ice, for 3 min. Sample was then centrifuged at 100,000 ×*g*, for 30 min, and the supernatant (containing membrane multiprotein complexes) was resolved by 1D-BN-PAGE. A schematic representation of the most important experimental steps used in this study is reported in Supplementary Fig. S1.

2.3. Electrophoresis

1D-BN-PAGE was carried out as described by Schagger and von Jagow [63], with some modifications. Different acrylamide gradients were tested to improve protein complex separation; thus, 4–14% and 7–14% linear gradients were used for final experiments. Anode buffer contained 50 mM Bis–Tris–HCl, pH 7, while cathode buffer was 15 mM Bis–Tris, 50 mM tricine, supplemented with 0.01% Coomassie Blue Brilliant G (Sigma). Before electrophoresis, samples were mixed with 0.1 vol of 100 mM Bis–Tris–HCl, pH 7.0, 30% (w/v) sucrose, 5% w/v Coomassie Blue Brilliant G and run in a mini-vertical unit (Hoefer Inc., Holliston, MA, USA) (110 × 100 mm, 0.75 mm thick) at 4 °C, by applying a constant voltage of 50 V, overnight, which was then gradually increased up to 200 V until completion. For visualization and further sampling for MS-based protein identification, gel lanes were stained using the blue–silver protocol [64]. Apparent molecular mass of bands was determined by using the NativeMark Unstained kit (Invitrogen Life Technologies, USA).

Non-stained gel lanes from 1D-BN-PAGE were cut out immediately and further subjected to a second dimension run by urea-PAGE or SDS-PAGE separation. For urea-PAGE, gel lanes were equilibrated in 6 M urea, 30% (w/v) glycerol, 4% (w/v) SDS, 2% (w/v) DTT, and 150 mM Tris–HCl, pH 6.8, for 15 min, and then reacted with 2.5% (w/v) iodoacetamide solved in the same buffer but depleted of the reducing agent, for additional 15 min. Gel lanes were then rinsed in equilibration buffer for 2 min and finally loaded onto the second dimension 12% T gel (1 mm thick). For SDS-PAGE, gel lanes were equilibrated in 150 mM Tris–HCl pH 6.8, containing 10% (w/v) glycerol, 2% (w/v) SDS, and 2% (w/v) DTT for 15 min, followed by a second incubation with the same buffer depleted of the reducing agent but containing 2.5% (w/v) iodoacetamide for 15 min. Gel lanes were then rinsed in equilibration buffer for 2 min and finally loaded onto the second dimension 9–16% T gradient gel (1 mm thick). In both cases, proteins were resolved at a constant current (25 mA) and visualized by using a blue–silver-based staining protocol [64].

2.4. Protein digestion and mass spectrometry analysis

Bands from 1D-BN-PAGE or spots from 2D-BN/urea-PAGE and 2D-BN/SDS-PAGE were manually excised from the gels, triturated and washed with water. Proteins were *in-gel* reduced, S-alkylated and digested with trypsin, as previously reported [65]. Protein digests were subjected to a desalting/concentration step on μZipTipC18 pipette tips (Millipore Corp., Bedford, MA, USA). Peptide mixtures were then analyzed by nLC–ESI-LIT-MS/MS using a LTQ XL mass spectrometer (ThermoFinnigan, USA) equipped with a Proxeon nanospray source connected to an Easy-nLC (Proxeon, Denmark) [66]. Peptide mixtures were separated on an Easy C18 column (100 × 0.075 mm, 3 μm) (Proxeon) using a gradient of acetonitrile containing 0.1% formic acid in aqueous 0.1% formic acid, at a flow rate of 300 nL/min; i) for spot identification, acetonitrile was ramped from 5% to 35% over 10 min, from 35% to 95% over 2 min and then remained at 95% over 12 min; ii) for band identification, acetonitrile was ramped from 5% to 40% over 40 min, from 35% to 80% over 10 min, from 80% to

95% over 2 min and then remained at 95% over 12 min. Spectra were acquired in the range *m/z* 400–2000. Acquisition was controlled by a data-dependent product ion scanning procedure over the three most abundant ions, enabling dynamic exclusion (repeat count 1 and exclusion duration of 1 min). The mass isolation window and collision energy were set to *m/z* 3 and 35%, respectively.

2.5. Protein identification

nLC–ESI-LIT-MS/MS data were searched by using Mascot (version 2.2.06) (Matrix Science, UK) and Sequest within Proteome Discoverer (version 1.3) software package (Thermo, USA) against an updated *S. thermophilus* database containing available protein sequences (NCBI 24/05/2012, 27333 sequences). As searching parameters, we used a mass tolerance value of 2 Da for precursor ion and 0.8 Da for MS/MS fragments, trypsin as proteolytic enzyme, a missed cleavages maximum value of 2, Cys carbamidomethylation and Met oxidation as fixed and variable modification, respectively. Protein candidates with more than 2 assigned unique peptides with an individual Mascot ion score >25 and a significant threshold ($p < 0.05$), and/or a Sequest X_{corr} value >1.5 (for +1), 2.0 (for +2) and 2.2 (for +3 and higher charges) were further considered for protein identification.

2.6. Bioinformatic analysis

Protein entries from spots in the same vertical line within 2D-BN/urea-PAGE or 2D-BN/SDS-PAGE, and in the corresponding band from 1D-BN-PAGE were analyzed by STRING v. 9.05 (http://string-db.org/), using *S. thermophilus* LMG18311 as selected organism. GO enrichment for biological processes, molecular functions and cellular components was also performed. The latter option was used to verify the occurrence of identified components as related to a membrane environment. Proteins or protein horthologs within each resulting STRING map were then searched against the eNet database (http://ecoli.med.utoronto.ca/index.php), or against combined MPIDB (http://jcvi.org/mpidb/about.php) [57], IntAct (http://www.ebi.ac.uk/intact) [59], DIP (http://dip.doe-mbi.ucla.edu/dip) [60] and BIOGRID (http://thebiogrid.org) database [61], using the service PSICQUIC interface (http://www.ebi.ac.uk/Tools/webservices/psicquic/view) [62]. This protocol was applied to all components as deriving from 1D-BN-PAGE, 2D-BN/urea-PAGE and 2D-BN/SDS-PAGE experiments, which were then critically evaluated according to available interaction information. A parallel analysis of each protein or protein hortholog for its oligomeric state as deriving from literature data or crystallographic information at PDB database (http://www.rcsb.org/pdb/home/home.do) was also performed. In this case, hortholog searching was performed by BLASTP analysis (http://blast.ncbi.nlm.nih.gov/Blast.cgi).

2.7. Eps and rgp gene clusters sequencing analysis

The sequence of *eps* and *rgp* gene clusters (accession HG321352 and HG321353) was obtained from a draft genome sequence of strain DSM20617. Partial genome sequencing was obtained from GenProbio s.r.l. (Codorago, Italy) by using the Ion Torrent PGM (Life Technologies, Germany). Functional annotation was performed by the Rapid Annotation using Subsystem Technology server [67] and checked by BLAST analysis [68] to verify and, if necessary, to redefine the start of each predicted coding region or to remove or add coding regions.

2.8. Analysis of exopolysaccharide production

Exopolysaccharide production was evaluated in ruthenium red milk (RRM) plates consisting of 0.5% w/v yeast extract, 10% w/v skim milk powder, 1% w/v sucrose, 1.5% w/v agar, and ruthenium red (0.08 g/L). Ruthenium red stains the bacterial cell wall producing red colonies for nonropy strains and white colonies for ropy strains [69,70].

Bacterial cells were collected by centrifugation, and the resulting pellet was processed for transmission electron microscopy. The extract treated bacterial cells were fixed in 2.5% glutaraldehyde, and later post-fixed with 1% osmium tetroxide (in 0.1 M cacodylate buffer, pH 7.2) for 2 h, at room temperature. After eliminating the remaining osmium tetroxide, the samples were dehydrated in a graduated cold ethanol series (35–100%); each step was performed for about 10–15 min, at room temperature. The fixed cells were embedded in Epon 812. Blocks were cut with an ultramicrotome (Ultracut; Reichert), and collected on nickel grids. Sections were post-stained with 5% uranyl acetate for 5 min at room temperature, and treated with lead citrate for 1 min. Sections were observed and photographed with a Philips CM 12 electron microscope and a Zeiss 900.

3. Results and discussion

3.1. Isolation and separation of membrane protein complexes

A global prediction of the membrane proteins within the *S. thermophilus* LMG18311 genome already identified 326 sequence entries containing at least one transmembrane helix (TMH) [7]; among that, 220 were predicted to contain more than 2 TMHs and 95 were clearly identified as transport system (TPS) components, which included 48 ATP-binding cassette (ABC) transporters, 29 secondary transporters, 7 ion channels, 6F- or P-type ATPases, and 2 sugar phosphotransferase systems (PTS) [7]. Within the ABC transporter group, 30 and 18 were classified as importers and exporters, respectively. Reduced content of sugar importers in *S. thermophilus* genome supported its low capacity for sugar uptake, with respect to other streptococci [6,7,69]. A high percentage of pseudogenes (20%) occurred within the transporter group. Other accessory factors involved in transport or membrane-associated components non-containing TMHs were also identified [7].

In order to optimize the preparation of membrane protein complexes from *S. thermophilus*, different detergents were tested. Those suitable for efficient extraction of membrane components often did not allow an optimal complex recovery (data not shown). Among non-ionic detergents (βDDM, digitonin and triton-X-100) tested, βDMM generated 1D-BN-PAGE profiles

showing the highest abundance of bands putatively ascribed to protein complexes. A further refinement of the concentration range of βDMM to be used for preparative membrane complex extraction was also obtained (Supplementary Fig. S2); thus, a concentration value of 0.5% (w/v) βDMM ensured a sufficient protein extraction power, together with a certain ability to resolve a number of protein complexes in a more or less intact form within a 60–720 kDa mass range. This guaranteed a high protein complex representation within 2D-BN/urea-PAGE and 2D-BN/SDS-PAGE maps (see below and data not shown); however, since each protein complex may have a diverse sensitivity to solubilization, we suggest to test various experimental conditions if it has to be fully characterized for its compositional/stoichiometric properties.

After initial resolution of the protein complexes by 1D-BN-PAGE, two complementary approaches (urea-PAGE and SDS-PAGE) were used for the separation in the second dimension (Figs. 1 and 2); in general, a reduced spot diffusion was observed in the first case. This combined procedure ensured confirmative data, but also provided complementary information for specific protein complexes. A similar condition was also verified by cross-relating data from 1D-BN-PAGE, 2D-BN/urea-PAGE and 2D-BN/SDS-PAGE experiments (Figs. 1 and 2); in fact, the first analysis highlighted the

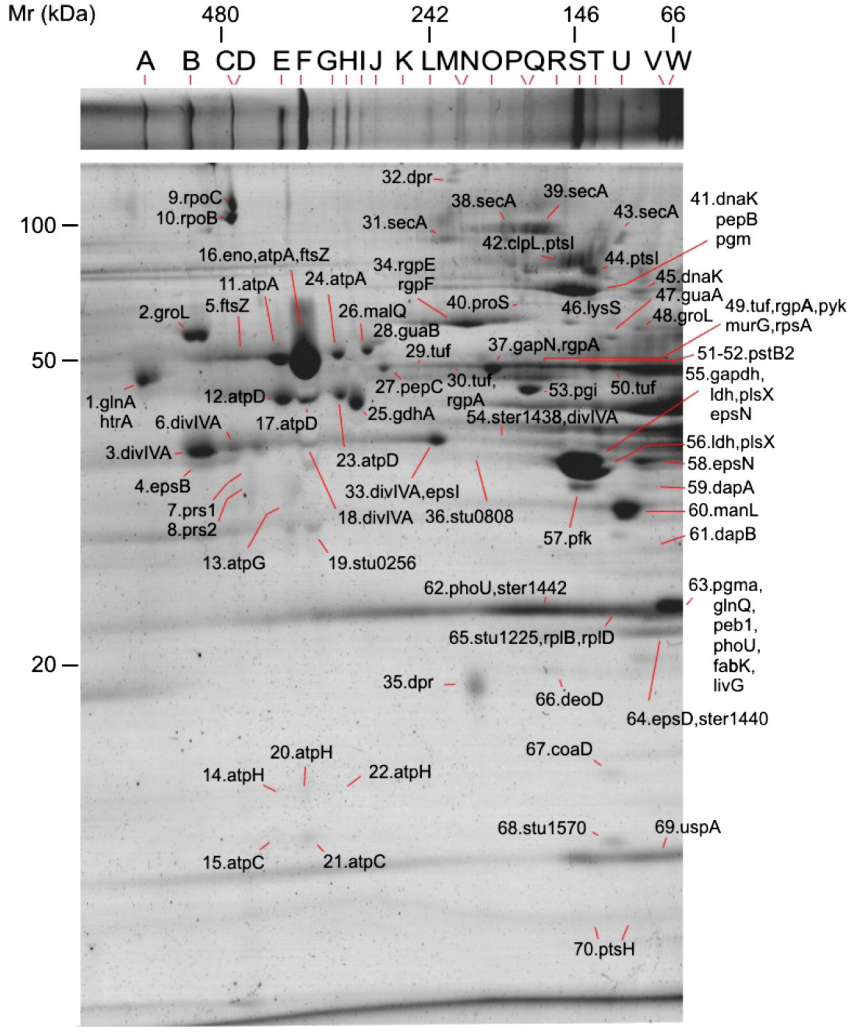

Fig. 1 – Top. 1D-BN-PAGE separation of membrane protein complexes from *Streptococcus thermophilus* strain DSM20617. About 100 μg of bacterial proteins were analyzed. Electrophoresis was performed on a gel casted with an acrylamide gradient of 4–14% T. Gels were stained by using a Coomassie blue–silver-based procedure. Commercially available molecular mass markers for the 1D-BN-PAGE are indicated at the top. Gel bands subjected to trypsinolysis and nLC–ESI-LIT-MS/MS analysis are indicated. Proteins identified by within each gel band are reported in Table 1 and Supplementary Table S1. Bottom. 2D-BN/urea-PAGE separation of membrane protein complexes from *Streptococcus thermophilus* strain DSM20617. About 50 μg of bacterial proteins were analyzed. The first dimension (BN-PAGE) was performed on a gel casted with an acrylamide gradient of 4–14% T; the second dimension (urea-PAGE) was performed on a gel casted with 12% T acrylamide. Gels were stained as mentioned above. Molecular mass markers for 1D-BN-PAGE and urea-PAGE are indicated at the top and on the left, respectively. Proteins identified by nLC–ESI-LIT-MS/MS are reported; identification details are specified in Supplementary Table S2. Corresponding heteromeric and homomeric protein complexes identified by combining 1D-BN-PAGE, 2D-BN/urea-PAGE and 2D-BN/SDS-PAGE experiments, followed by nLC–ESI-LIT-MS/MS analysis, are shown in Table 1.

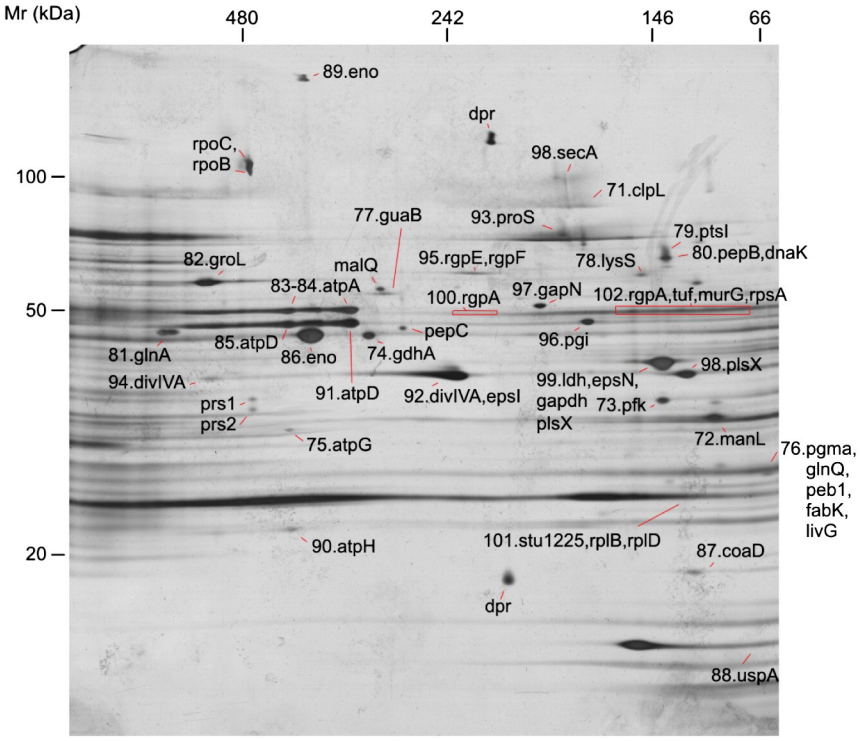

Fig. 2 – 2D-BN/SDS-PAGE separation of membrane protein complexes from *Streptococcus thermophilus* strain DSM20617. About 50 μg of bacterial proteins were analyzed. The first dimension (BN-PAGE) was performed on a gel casted with an acrylamide gradient of 7–14% T; the second dimension (SDS-PAGE) was performed on a gel casted with an acrylamide gradient of 9–16% T. Gels were stained by using a Coomassie blue–silver-based procedure. Molecular mass markers for 1D-BN-PAGE and urea-PAGE are indicated at the top and on the left, respectively. Proteins identified by nLC–ESI-LIT-MS/MS are indicated; identification details are reported in Supplementary Table S3. Corresponding heteromeric and homomeric protein complexes identified by combining 1D-BN-PAGE, 2D-BN/urea-PAGE and 2D-BN/SDS-PAGE, followed by nLC–ESI-LIT-MS/MS analysis, are shown in Table 1.

occurrence of minor protein components that were not sampled in the 2D maps (as result of their migration in faint, diffused spots) or were absent therein as result of their poor solubility within the PAGE matrix. Synergic effect of combining data from 1D and 2D-BN-PAGE has been already underlined in previous studies on complexomes from other prokaryotes and eukaryotes [41,43,49,54,55,71]. Protein information on spots from 2D-BN/urea-PAGE or 2D-BN/SDS-PAGE, and bands from 1D-BN-PAGE always derived from nLC–ESI-LIT-MS/MS analysis of the corresponding *in gel* tryptic digests. In general, 1D-BN-PAGE ensured a higher number of identified proteins with respect to 2D-BN/urea-PAGE and 2D-BN/SDS-PAGE; this was probably the result of the higher amount of sample loaded for analysis and/or the absence of a second dimension separation. For evaluation/interpretation of the whole experimental results, an integration of 1D-BN-PAGE migration and MS-based identification data with available protein interaction and oligomerization information in other bacteria was achieved. Altogether, these integrated experiments allowed describing 65 heteromeric and 30 homomeric protein complexes where a total of 110 gene expression products were present (Table 1).

A *post-hoc* evaluation of the nature of the proteins identified from 1D-BN-PAGE, 2D-BN/urea-PAGE and 2D-BN/SDS-PAGE experiments generally demonstrated negligible cytoplasmic contaminations, as revealed by the absence of abundant cytosolic proteins already identified in previous dedicated studies on *S. thermophilus*, i.e. transcription elongation factor NusA, Mn-dependent inorganic pyrophosphatase and most ribosomal particle constituents [13,14]. In parallel, various moonlighting proteins were also identified; their occurrence in membranes has been already reported in other bacteria [72,73]. In general, our analysis described a number of protein complexes that are representative of the most important functional modules within the cell membrane. Protein machineries involved in polysaccharide biosynthesis, molecular uptake, energy metabolism, cell division, protein secretion, folding and chaperone activity were highly represented in 1D-BN-PAGE, 2D-BN/urea-PAGE and 2D-BN/SDS-PAGE profiles; a number of homomeric moonlighting proteins were also identified. Their properties will be discussed in detail in the following sections, here organized according to a functional criterion.

3.2. *Exopolysaccharide biosynthesis*

The ability of *S. thermophilus* to produce exopolysaccharide (EPS) is important for the dairy industry, as it enhances the texture and mouthfeel of certain fermented dairy products. EPS is highly variable among *S. thermophilus* strains and

consists of heterosaccharide polymers primarily made of galactose, glucose and rhamnose monomers [74,75]. EPS biosynthesis in *S. thermophilus* involves binding of sugar monomers to a lipid carrier, using amino sugars as precursors. This reaction is performed by a galactose-1-phosphate or glucose-1-phosphate transferase, and subsequent attachment of different monomers is performed by glycosyl transferases. In addition to this, enzymes for polymerization and transmembrane translocation are needed [75,76]. Coding genes for these enzymes are arranged into a main EPS cluster, which generally contains 12–25 gene entries and shows an extremous degree of variability among different bacterial strains [8,69,74,77]; thus, more than 60 different *S. thermophilus* EPS gene clusters have been predicted by restriction fragment length polymorphism analysis [78]. The modular gene organization is conserved in all EPS clusters and the biosynthesis of EPS is proposed to occur via a common molecular mechanism. Interestingly, the *S. thermophilus* genome also contains a second gene cluster predicted to be involved in rhamnose–glucose polysaccharide (RGP) production. Six conserved genes (*rgpA–F*) (including two ones coding for molecular ABC exporter components) determine the assembly and secretion of the rhamnose–glucose polysaccharide, while two or more variable genes located upstream (*rgpH–I*) are required for glucose side-chain coupling, controlling the frequency of branching [7,79]. Many aspects of polysaccharide biosynthesis are still not fully understood, such as the sequence similarity of some enzymes involved in EPS and RGP assemblage, or their eventual, concomitant occurrence in functionally-active machineries.

In this study, a number of protein complexes made of both *eps* and *rgp* gene products were observed; additional complexes made only of *eps*-coded enzymes were also identified. In particular, epsB–epsC, rgpA–rgpD–rgpE–rgpF–epsI–epsJ, rgpA–rgpD–rgpE–rgpF–epsI, rgpA–rgpD–rgpF–epsI–ster1438, rgpA–rgpD–rgpF–epsI, rgpA–rgpD–rgpF–ster1438, epsG–epsI–epsJ–epsN–ster1442, epsI–epsJ–epsN–ster1442, rgpA–epsG–epsI, epsD–epsN–ster1440 and rgpA–epsI complexes were characterized by combining MS data of samples from 1D-BN-PAGE, 2D-BN/urea-PAGE and 2D-BN/SDS-PAGE (Fig. 1 and Table 1). Protein components were identified as deriving from different *S. thermophilus* strains; their nature strongly reflected the high variability of the corresponding EPS clusters and the absence of genomic information on the DSM20617 strain. Protein redundancies were excluded on the basis of sequence alignment of all identified species. In some cases, complex nature reflected progressive decomposition of higher structures. Generally, their molecular mass value was in good agreement with that expected theoretically. Exceptions regarded poorly-represented epsB–epsC-containing complexes at 602 and 518 kDa, for which the occurrence of additional constituents (in low amounts) escaping a positive MS identification may be hypothesized, as already reported for other poorly-abundant protein complexes from other bacteria [44,45,52,55,57].

To further investigate the arrangement of the genes coding for the proteins reported above in the corresponding clusters and to verify the sequence of those coding for ster-related entries, a successive, dedicated analysis was performed on strain DSM20617. Partial genome sequencing revealed that the EPS locus is composed of 13 genes and one pseudogene (*epsH**) (Fig. 3A), which show a high sequence identity (93–99%) with counterparts from the *S. thermophilus*/*Streptococcus salivarius*/*Streptococcus vestibularis* group. Concerning the gene organization in the EPS locus, only the first part of the cluster (*eps*ABCDE) appeared as highly conserved among *S. thermophilus* strains. Complessively, the entire EPS locus showed a gene order highly similar to that of *Streptococcus mitis* NCTC 1, despite a low sequence identity. On the other hand, the RGP locus was composed of 14 genes showing high sequence similarity (99–100%) with orthologs from *S. thermophilus* and *Streptococcus parasanguinis* strains (Fig. 3B). Both EPS and the RGP loci showed a low GC content (36 and 37% respectively) if compared to that of the whole genome GC (39%), thus suggesting a potential role of horizontal gene transfer events in the acquisition/assembly of these gene clusters.

On the basis on the results reported above, it was possible to ascertain that a number of enzymes coded from genes present in the same cluster establish positive interactions to each other (Table 1 and Fig. 3). Their identification in the βDMM-extracted fraction was suggestive for the occurrence of two dedicated biosynthetic machineries as embedded into the lipid bilayer to ensure trafficking of the assembled sugar oligomers from the inner side of the cell membrane toward the bacterial surface, for its incorporation in the bacterial capsular structures or its eventual release in the medium. Our results confirmed previous data on epsB–epsC–epsD binding in *S. thermophilus* and other pathogenic streptococci, as deriving from co-purification, co-immunoprecipitation or two-hybrid assays [76,80] but, at the same time, they also highly expanded the interaction maps of exopolysaccharide biosynthesis enzymes [76,81–83]. On the other hand, the simultaneous occurrence of mixed gene products from EPS and RGP clusters onto independent protein machineries having putative separate oligosaccharide translocation mechanism across membranes was never reported so far; it was highly suggestive of a hierarchical organization of the complexes into a unique, synchronized, functional biosynthetic module. In this context, the occurrence of genes coding for proteins involved in the synthesis of the dTDP-rhamnose precursor has been already demonstrated in the EPS cluster of different pathogenic streptococci and lactobacilli [76,79,84,85], evocating a sort of genetic cross-talk between the corresponding rhamnose- and galactose/glucose-based biosynthetic machineries [75,76]. On the other hand, the functionality of the whole exopolysaccharide biosynthesis module in *S. thermophilus* DSM20617 was confirmed by a ruthenium red stain assay, which revealed white colonies (unstained) on agar plate (Fig. 4A), and by previous data [74]. Transmission electron microscopy confirmed the presence of a diffuse polysaccharide matrix on the surface of the bacterial cells (Fig. 4B and C), highly similar to that reported for the closest neighbor *L. lactis* [79]. On the whole, our results can provide original insights for future studies on EPS production in lactic acid bacteria.

3.3. *Solute transport systems*

A number TMH-containing proteins and TPS components, including ion channels, secondary transporters, sugar PTSs, ABC transporters and ATP synthases, were recognized as constituents of protein complex structures present within distinct bands from 1D-BN-PAGE or as vertical lines of spots in 2D-BN/urea-PAGE and 2D-BN/SDS-PAGE (Figs. 1 and 2). Among

Table 1 – Protein heteromultimeric and homomeric complexes identified in the membrane fraction of exponentially-growing *Streptococcus thermophilus* cells. Band in 1D-BN-PAGE, protein complex experimental migration (as deduced with respect to commercial molecular standards), protein complex description, corresponding protein name, gene name in the LMG18311 or LMD-9 genome [6,8], accession number, theoretical Mr value, number of observed unique peptides, sequence coverage and identification score are listed. Identification data reported in this table are those with the highest values as obtained from 1D-BN-PAGE (Fig. 1), 2D-BN/urea-PAGE (Fig. 1) and 2D-BN/SDS-PAGE (Fig. 2). Protein components identified in spots from 2D-BN/urea-PAGE and 2D-BN/SDS-PAGE are indicated with an asterisk and circle, respectively. MS details for the identification data reported in this table are available in Supplementary Table S1 (for 1D-BN-PAGE), Supplementary Table S2 (for 2D-BN/urea-PAGE) and Supplementary Table S3 (for 2D-BN/SDS-PAGE).

Band	Complex migration (kDa)	Protein complex	Protein name	Gene name	Accession	Mass (kDa)	Unique peptides	Sequence coverage (%)	Mascot score
A	602	GlnA (dodecamer)	Glutamine synthetase type I — GlnA*° [c]	Stu1776	54306535	50.1	14	38.26	528
		Stu0296–Stu0297	Amino acid ABC transporter substrate-binding protein — Stu0296 [a,b]	Stu0296	55822277	31.3	2	9.22	115
			Amino acid ABC transporter substrate-binding protein — Stu0297 [a,b]	Stu0297	55822278	32.9	4	9.67	58
		LmrA1–LmrA2	ABC-type multidrug (DrugE2) exporter system, ATPase and permease component — LmrA1 [a]	Stu0433	116627330	67.1	6	13.41	134
			Multidrug ABC exporter ATP binding/membrane-spanning protein — LmrA2 [a]	Stu0434	55820521	65.1	3	6.42	98
		HtrA–LacS	Trypsin-like serine protease — HtrA* [b]	Stu2024	116628681	42.8	3	14.36	175
			Lactose permease — LacS [a]	Stu1398	38492233	69.1	5	8.68	118
		HtrA–ScrA	Trypsin-like serine protease — HtrA* [b]	Stu2024	116628681	42.8	2	14.36	175
			Sucrose PTS, EIIBCA — ScrA [a]	Stu1734	116628430	66.9	3	6.32	78
		EpsB–EpsC	Glycosyl transferase family protein — EpsB* [c]	Stu1485	55823391	35.0	6	17.53	121
			Exopolysaccharide synthesis protein 4C — EpsC [a]	Stu1110	24637401	25.5	3	13.91	6.62 [d]
B	518	FtsZ–EzrA–DivIVA–MurG	Cell division protein FtsZ — FtsZ* [c]	Stu0735	55822702	46.5	3	7.50	100
			Septation ring formation regulator EzrA — EzrA [c]	Stu1520	116628215	61.5	2	4.33	83
			Cell division initiation protein — DivIVA* [c]	Stu0740	116627610	33.0	14	37.11	515
			UDP-N-acetylglucosamine-N-acetylmuramyl-(pentapeptide) pyrophosphoryl-undecaprenol N-acetylglucosamine transferase — MurG [c]	Stu0732	81559554	40.1	3	11.80	66
		GroL (homomer)	60 kDa chaperonin — GroL*° [c]	Stu0204	68566260	56.9	16	53.06	775
		EpsB–EpsC	Glycosyl transferase family protein — EpsB* [c]	Stu1485	55823391	35.0	2	6.82	128
			Exopolysaccharide synthesis protein 4C — EpsC [a]	Stu1110	24637493	25.5	4	19.13	94
		Stu0296–Stu0297	Amino acid ABC transporter substrate-binding protein — Stu0296 [a]	Stu0296	55822277	31.3	2	9.22	93
			Amino acid ABC transporter substrate-binding protein — Stu0297 [a]	Stu0297	55822278	32.9	3	5.67	50
C	446	FtsZ–DivIVA–MurG	Cell division protein FtsZ — FtsZ* [c]	Stu0735	55822702	46.5	3	10.00	152
			Cell division initiation protein — DivIVA*° [c]	Stu0740	116627610	33.0	3	17.18	190
			UDP-N-acetylglucosamine-N-acetylmuramyl-(pentapeptide) pyrophosphoryl-undecaprenol N-acetylglucosamine transferase — MurG [c]	Stu0732	81559554	40.1	4	15.17	82
		Prs1–Prs2	Ribose-phosphate pyrophosphokinase — Prs1*° [c]	Stu0023	116626993	35.1	4	17.76	125
			Ribose-phosphate pyrophosphokinase — Prs2*° [c]	Stu1460	116628164	35.1	4	19.81	112
		RpoA–RpoB–RpoC	DNA-directed RNA polymerase subunit alpha — RpoA [c]	Stu1908	81558875	34.4	2	7.37	4.16 [d]
			DNA-directed RNA polymerase subunit beta — RpoB*° [c]	Stu1868	55821840	133.3	3	3.27	195
			DNA-directed RNA polymerase subunit beta′ — RpoC*° [c]	Stu1867	55821839	135.3	3	2.55	118
		FtsH (hexamer)	Cell division protein FtsH — FtsH [c]	Stu0012	116626986	71.9	3	4.73	7.26 [d]
D	433	FtsZ–EzrA–DivIVA	Cell division protein FtsZ — FtsZ* [c]	Stu0735	55822702	46.5	4	10.91	177
			Septation ring formation regulator EzrA — EzrA [c]	Stu1520	55821496	65.4	2	3.90	51
			Cell division initiation protein — DivIVA* [c]	Stu0740	116627610	33.0	3	11.34	129

(continued on next page)

Table 1 (*continued*)

Band	Complex migration (kDa)	Protein complex	Protein name	Gene name	Accession	Mass (kDa)	Unique peptides	Sequence coverage (%)	Mascot score
E	403	ATPase A–ATPase C–ATPase D–ATPase G–ATPase H	H^+-ATPase cytoplasmic F1-part alpha subunit — ATPase A*° [a]	Stu0482	20070091	54.5	4	25.55	300
			H^+-ATPase cytoplasmic F1-part epsilon subunit — ATPase C* [a]	Stu0485	20070094	5.2	2	56.25	72
			ATP synthase F1-sector beta subunit — ATPase D*° [a]	Stu0484	81820338	50.8	18	55.56	1103
			ATP synthase F1-sector gamma subunit — ATPase G*° [a]	Stu0483	81676597	32.2	7	27.05	164
			ATP synthase F1-sector delta subunit — ATPase H*° [a]	Stu0481	81559722	20.4	3	13.48	129
F	371	Eno (octamer)	Enolase — Eno*° [c]	Stu0635	68053529	47.0	32	89.63	1688
		ATPase A–ATPase C–ATPase D–ATPase H	H^+-ATPase cytoplasmic F1-part alpha subunit — ATPase A*° [a]	Stu0482	20070091	54.5	2	13.97	186
			ATP synthase F0F1 subunit epsilon — ATPase C* [a]	Stu0485	55820568	16.7	2	21.62	88
			ATP synthase F1-sector beta subunit — ATPase D*° [a]	Stu0484	81820338	50.8	8	22.86	298
			ATP synthase F1-sector delta subunit — ATPase H* [a]	Stu0481	81559722	20.4	3	19.66	98
		FtsZ–DivIVA	Cell division protein FtsZ — FtsZ* [c]	Stu0735	55822702	46.5	3	9.77	100
			Cell division initiation protein — DivIVA* [c]	Stu0740	116627610	33.0	4	10.65	116
		RpoB–RpoC–Stu0256	DNA-directed RNA polymerase subunit beta — RpoB [c]	Stu1868	55821840	133.3	3	3.02	103
			DNA-directed RNA polymerase subunit beta′ — RpoC [c]	Stu1867	122266859	135.2	2	1.73	3.67 [d]
			Non-canonical purine NTP pyrophosphatase — Stu0256	Stu0256	62900158	36.0	4	16.67	140
G	333	ATPase A–ATPase D–ATPase H	H^+-ATPase cytoplasmic F1-part alpha subunit — ATPase A*° [a]	Stu0482	20070091	54.5	3	33.33	607
			ATP synthase F1-sector beta subunit — ATPase D*° [a]	Stu0484	81820338	50.8	23	68.16	1636
			ATP synthase F1-sector delta subunit — ATPase H* [a]	Stu0481	122268026	20.4	4	23.60	140
H	318	GdhA (hexamer)	Glutamate dehydrogenase — GdhA*° [c]	Stu0430	116627327	48.3	30	74.00	1456
		ClpL (tetramer)	ATP-dependent proteinase ATP-binding subunit — ClpL	Stu1614	55821590	77.1	7	15.45	249
I	303	MalQ (homomer)	4-Alpha-glucanotransferase — MalQ*°	Stu1013	116627804	56.6	17	34.28	492
		FtsZ–MurG–Pbp2X–SecA–Tuf	Cell division protein FtsZ — FtsZ [c]	Stu0735	55822702	46.5	5	10.68	132
			UDP-N-acetylglucosamine-N-acetylmuramyl-(pentapeptide) pyrophosphoryl-undecaprenol N-acetylglucosamine transferase — MurG [c]	Stu0732	122267800	40.2	2	7.58	4.69 [d]
			Cell division protein FtsI/penicillin binding protein 2X — Pbp2X [b]	Stu1701	116628388	82.6	2	3.44	4.08 [d]
			Protein translocase subunit SecA — SecA [a]	Stu1730	122266980	96.3	2	2.12	4.28 [d]
			Elongation factor Tu — Tuf [c]	Stu0487	81559720	43.8	3	9.05	72
J	288	GuaB–UvrB	Inosine 5′-monophosphate dehydrogenase — GuaB*°	Stu2016	55821983	52.9	2	6.09	75
			UvrABC system protein B, excinuclease ABC subunit B — UvrB	Stu1497	122267209	76.6	2	4.49	4.26 [d]
		PepC (hexamer)	Aminopeptidase C – PepC*° [c]	Stu0229	3024365	50.4	12	28.54	278
		SecA–FtsY–PrtM	Protein translocase subunit SecA — SecA [a]	Stu1730	122266980	96.3	4	5.65	111
			Signal recognition particle receptor (docking protein) — FtsY [a]	Stu1432	116628140	51.0	2	5.18	79
			Protease maturation protein precursor — PrtM [b]	Stu0456	55822430	39.9	2	7.82	79
K	261	Tuf–GroL–ClpL–PotA	Elongation factor Tu — Tuf* [c]	Stu0487	81559720	43.8	3	6.78	98
			60 kDa chaperonin — GroL [c]	Stu0204	68566260	56.9	3	5.75	63
			ATP-dependent proteinase ATP-binding subunit — ClpL	Stu1614	116628305	77.1	4	8.01	141
			Spermidine/putrescine import ATP-binding protein PotA — PotA [a]	Stu1538	122267176	43.8	2	5.99	72
L	243	FtsZ–DivIVA–SecA–PrtM–Tuf	Cell division protein FtsZ — FtsZ [c]	Stu0735	55822702	46.5	4	12.73	121
			Cell division initiation protein — DivIVA*° [c]	Stu0740	116627610	33.0	17	36.08	508
			Protein translocase subunit SecA — SecA* [a]	Stu1730	122266980	96.3	15	20.85	405
			Protease maturation protein precursor — PrtM [b]	Stu0456	55822430	39.9	3	9.43	105
			Elongation factor Tu — Tuf* [c]	Stu0487	81559720	43.8	7	24.12	302

		RgpA/EpsF–RgpD–RgpE–RgpF–EpsI–EpsJ	Polysaccharide biosynthesis protein EpsF — RgpA/EpsF*° [c]	Stu1472	90655845	44.5	2	6.67	58	
			ABC-type polysaccharide/polyol phosphate transport system, ATPase component — RgpD [a]	Stu1469	116628173	44.6	6	13.25	67	
			Glycosyltransferase — RgpE*°	Stu1468	116628172	66.1	14	25.79	291	
			Polysaccharide biosynthesis protein — RgpF*°	Stu1467	116628171	68.4	4	8.09	91	
			Polysaccharide biosynthesis protein — EpsI*° [c]	–	24637447	38.2	2	7.01	5.90 [d]	
			Polysaccharide biosynthesis protein — EpsJ [c]	–	24637448	38.7	2	5.76	3.98 [d]	
		RpoC–RplJ–RplS	DNA-directed RNA polymerase subunit beta′ — RpoC [c]	Stu1867	122266859	135.2	2	1.73	3.67 [d]	
			50S ribosomal protein L10 — RplJ	Stu0536	97182027	17.5	2	13.17	64	
			50S ribosomal protein L19 — RplS	Stu1179	62287370	13.1	2	20.87	4.75 [d]	
M	222	FtsZ–DivIVA–MurG–Pbp2X–Tuf	Cell division protein FtsZ — FtsZ [c]	Stu0735	55822702	46.5	3	9.32	132	
			Cell division initiation protein — DivIVA°[c]	Stu0740	116627610	33.0	3	12.71	96	
			UDP-N-acetylglucosamine-N-acetylmuramyl-(pentapeptide) pyrophosphoryl-undecaprenol N-acetylglucosamine transferase — MurG [c]	Stu0732	122267800	40.2	2	7.02	5.32 [d]	
			Cell division protein FtsI/penicillin binding protein 2X — Pbp2X [b]	Stu1701	116628388	82.6	2	3.44	3.8 [d]	
			Elongation factor Tu — Tuf [c]	Stu0487	81559720	43.8	12	39.95	377	
		Dpr (dodecamer)	Peroxide resistance protein, non-heme iron-containing ferritin — Dpr*° [c]	Stu0723	116627595	19.2	7	38.73	386	
		Stu0808–stu0809	Hypothetical protein — Stu0808* [b]	Stu0808	55822775	35.6	4	12.80	88	
			Carbohydrate ABC uptake transporter ATP-binding protein — Stu0809 [a]	Stu0809	116627673	55.5	2	4.10	91	
N	216	Dpr (dodecamer)	Peroxide resistance protein, non-heme iron-containing ferritin — Dpr*° [c]	Stu0723	116627595	19.2	7	38.73	386	
		RgpA/EpsF–RgpD–RgpE–RgpF–EpsI	Polysaccharide biosynthesis protein EpsF — RgpA/EpsF* [c]	Stu1472	24637426	44.6	2	6.67	72	
			ABC-type polysaccharide/polyol phosphate transport system, ATPase component — RgpD [a]	Stu1469	116628173	44.6	9	30.75	238	
			Polysaccharide biosynthesis protein/glycosyltransferase — RgpE*	Stu1468	55823378	66.0	6	12.30	82	
			Polysaccharide biosynthesis protein — RgpF*	Stu1467	116628171	68.4	8	18.07	156	
			Polysaccharide biosynthesis protein — EpsI [c]	–	24637447	38.2	4	13.72	84	
		Tuf–RpsA–FusA–DnaK	Elongation factot Tu — Tuf* [c]	Stu0487	81559720	43.8	9	29.65	230	
			30S ribosomal protein S1 — RpsA* [c]	Stu0592	161936373	43.9	15	40.75	430	
			Elongation factor G — FusA [c]	Stu1789	62286650	76.6	5	10.10	164	
			Chaperon protein DnaK — DnaK* [c]	Stu0120	81676627	64.8	18	34.27	467	
O	196	PurB (tetramer)	Adenylosuccinate lyase — PurB [c]	Stu0045	55822037	49.5	4	11.34	7.68 [d]	
		Als (tetramer)	Acetolactate synthase — Als	Stu0923	20976803	52.3	2	4.61	62	
		ManL–ManM–ManN	Mannose PTS system component IIAB — ManL [a]	Stu0333	30027111	35.8	2	7.58	72	
			Mannose PTS system component IIC — ManM [a]	Stu0332	55820425	27.8	3	12.36	136	
			Mannose PTS system component IID — ManN [a]	Stu0331	55820424	33.5	3	12.21	7.06 [d]	
		FtsZ–DivIVA–SecA–FtsY	Cell division protein FtsZ — FtsZ [c]	Stu0735	55822702	46.5	3	8.86	129	
			Cell division initiation protein — DivIVA* [c]	Stu0740	116627610	33.0	2	7.22	52	
			Protein translocase subunit SecA — SecA* [a]	Stu1730	122266980	96.3	4	5.42	67	
			Signal recognition particle receptor (docking protein) — FtsY [a]	Stu1432	116628140	51.0	2	5.18	5.18 [d]	
		GapN (tetramer)	NADP-dependent glyceraldehyde-3-phosphate dehydrogenase — GapN*° [c]	Stu1263	116628006	50.8	20	55.14	870	
		RgpA/EpsF–RgpD–RgpF–EpsI–Ster1438	Polysaccharide biosynthesis protein EpsF — RgpA/EpsF* [c]	Stu1472	24637479	44.7	4	12.05	115	
			ABC-type polysaccharide/polyol phosphate transport system, ATPase component — RgpD [a]	Stu1469	116628173	44.6	12	32.00	243	
			Polysaccharide biosynthesis protein — RgpF*	Stu1467	116628171	68.4	6	13.43	128	
			Polysaccharide biosynthesis protein — EpsI [c]	–	24637447	38.2	5	14.02	79	
			Cell wall biosynthesis glycosyltransferase — Ster1438* [c]	Ster1438	116628177	30.3	7	26.36	197	
P	171	SecA–FtsY–Ffh	Protein translocase subunit SecA — SecA*° [a]	Stu1730	122266980	96.3	6	9.89	379	
			Signal recognition particle receptor (docking protein) — FtsY [a]	Stu1432	116628140	51.0	3	10.15	120	

(continued on next page)

Table 1 (*continued*)

Band	Complex migration (kDa)	Protein complex	Protein name	Gene name	Accession	Mass (kDa)	Unique peptides	Sequence coverage (%)	Mascot score
			Signal recognition particle protein — Ffh[a]	Stu0889	55822851	57.9	2	6.35	5.63[d]
		MurE–MurG–MurM–Pbp2X	Mur ligase — MurE	Stu1254	116627998	48.7	14	38.32	351
			UDP-N-acetylglucosamine-N-acetylmuramyl-(pentapeptide) pyrophosphoryl-undecaprenol N-acetylglucosamine transferase — MurG*°[c]	Stu0732	122267800	40.2	9	30.9	192
			Peptidoglycan branched peptide synthesis protein, alanine adding enzyme — MurM[c]	Stu1155	13324647	46.2	20	52.23	820
			Cell division protein FtsI/penicillin binding protein 2X — Pbp2X[b]	Stu1701	116628388	82.6	2	3.97	4.62[d]
		Pyk (tetramer)	Pyruvate kinase — Pyk[c]	Stu1196	161936368	54.5	7	17.80	215
		RgpA/EpsF–RgpD–RgpF–EpsI	Polysaccharide biosynthesis protein EpsF — RgpA/EpsF*°[c]	Stu1472	90655845	44.5	7	22.31	239
			ABC-type polysaccharide/polyol phosphate transport system, ATPase component — RgpD[a]	Stu1469	116628173	44.6	10	26.25	217
			Polysaccharide biosynthesis protein — RgpF*	Stu1467	116628171	68.4	4	8.43	83
			Polysaccharide biosynthesis protein — EpsI[c]	–	24637447	38.2	5	18.60	69
		PstB2	ABC-type phosphate transport system, ATPase component — PstB2*[a]	Stu1005	116627797	28.0	3	12.70	118
		TpiA–Pfl	Triosephosphate isomerase, TpiA[c]	Stu0488	17066728	26.7	5	25.40	243
			Pyruvate formate-lyase, Pfl	Stu1657	55823561	87.0	3	4.42	94
Q	167	DivIVA–MurG–SecA	Cell division initiation protein — DivIVA*[c]	Stu0740	116627610	33.0	17	36.08	508
			UDP-N-acetylglucosamine-N-acetylmuramyl-(pentapeptide) pyrophosphoryl-undecaprenol N-acetylglucosamine transferase — MurG*°[c]	Stu0732	122267800	40.2	6	16.29	177
			Protein translocase subunit SecA*°[a]	Stu1730	122266980	96.3	15	23.67	448
		ProS (dimer)	Proline-tRNA ligase — ProS*°	Stu0200	81820361	69.1	20	40	514
		Pgi–MetN	Glucose-6-phosphate isomerase — Pgi*°[c]	Stu0194	81170506	49.8	14	38	497
			Methionine import ATP-binding protein — MetN[a]	Stu0301	81820355	38.7	3	9.58	7.35[d]
		DnaK–RpsA–ClpL	Chaperon protein DnaK — DnaK*[c]	Stu0120	81676627	64.8	10	22.41	218
			30S ribosomal protein S1 — RpsA*°[c]	Stu0592	161936373	43.9	7	20.75	164
			ATP-dependent proteinase ATP-binding subunit — ClpL*°	Stu1614	55823518	77.1	34	50.36	2165
		RgpA/EpsF–RgpD–RgpF–Ster1438	Polysaccharide biosynthesis protein EpsF — RgpA/EpsF*°[c]	Stu1472	116628176	44.0	5	18.85	120
			ABC-type polysaccharide/polyol phosphate transport system, ATPase component — RgpD[a]	Stu1469	116628173	44.6	2	5.25	70
			Polysaccharide biosynthesis protein — RgpF*	Stu1467	116628171	68.4	3	6.54	68
			Cell wall biosynthesis glycosyltransferase — Ster1438*[c]	Ster1438	116628177	30.3	7	26.36	197
R	146	MurE–MurG–MurM–Upps	Mur ligase — MurE	Stu1254	55823172	49.4	18	43.85	549
			UDP-N-acetylglucosamine-N-acetylmuramyl-(pentapeptide) pyrophosphoryl-undecaprenol N-acetylglucosamine transferase — MurG*°[c]	Stu0732	122267800	40.2	5	18.54	190
			Peptidoglycan branched peptide synthesis protein, alanine adding enzyme — MurM[c]	Stu1155	13324647	46.2	16	40.84	557
			Isoprenyl transferase — Upps	Stu0197	73920281	28.7	3	12.05	100
		Ffh–FusA–Tuf	Signal recognition particle protein — Ffh[a]	Stu0889	55822851	57.9	2	6.35	5.63[d]
			Elongation factor G — FusA[c]	Stu1789	62286650	76.6	2	3.32	79
			Elongation factor Tu — Tuf*°[c]	Stu0487	81559720	43.8	3	9.30	64
		EpsG–EpsI–EpsJ–EpsN–Ster1442	Polysaccharide biosynthesis protein — EpsG[c]	–	24637427	42.6	2	7.61	60
			Polysaccharide biosynthesis protein — EpsI[c]	–	24637447	38.2	3	9.45	89
			Polysaccharide biosynthesis protein — EpsJ[c]	–	24637448	38.7	2	5.76	4.45[d]
			Polysaccharide biosynthesis protein — EpsN*°[c]	–	24637452	39.0	2	7.43	100

			Cell wall biosynthesis glycosyltransferase — Ster1442*[c]	Ster1442	116628181	37.5	5	16.92	81
		DnaK–RpsA–Pyk	Chaperon protein DnaK — DnaK*[c]	Stu0120	81676627	64.8	44	64.91	1442
			30S ribosomal protein S1 — RpsA*°[c]	Stu0592	161936373	43.9	9	29.25	159
			Pyruvate kinase — Pyk*°[c]	Stu1196	116627931	54.5	10	21.60	318
S	131	PepB (dimer)	Oligopeptidase — PepB*°	Stu0454	116627347	69.2	5	7.99	107
		DeoD (hexamer)	Purine nucleoside phosphorylase — DeoD*[c]	Stu1113	24473734	18.2	3	24.54	171
		Pgm (dimer)	Phosphoglucomutase — Pgm*	Stu0787	116627655	63.1	4	7.17	69
		LysS–PlsX–SerS	Lysine-tRNA ligase — LysS*°	Stu0692	122267836	56.4	8	16.13	229
			Phosphate acyltransferase — PlsX*°[c]	Stu0028	122268399	35.5	5	14.67	108
			Serine-tRNA ligase — SerS	Stu0329	122268151	48.0	3	9.18	9.11[d]
		PhoU–PstB2–FtsZ–Tuf	Phosphate uptake regulatory protein — PhoU*[c]	Stu1006	55737024	24.9	2	9.63	57
			ABC-type phosphate transport system, ATPase component — PstB2*[a]	Stu1005	55821038	28.0	3	15.47	85
			Cell division protein FtsZ — FtsZ[c]	Stu0735	55822702	46.5	2	6.59	67
			Elongation factor Tu — Tuf*°[c]	Stu0487	81559720	43.8	11	35.68	506
		EpsI–EpsJ–EpsN–Ster1442	Polysaccharide biosynthesis protein — EpsI[c]	–	24637447	38.2	9	27.74	241
			Polysaccharide biosynthesis protein — EpsJ[c]	–	24637448	38.7	5	13.03	160
			Polysaccharide biosynthesis protein — EpsN*°[c]	–	24637452	39.0	7	21.14	282
			Cell wall biosynthesis glycosyltransferase — Ster1442*[c]	Ster1442	116628181	37.5	3	9.54	54
T	118	RpsA–ClpL	30S ribosomal protein S1 — RpsA*[c]	Stu0592	161936373	43.9	7	19.50	202
			ATP-dependent proteinase ATP-binding subunit – ClpL*	Stu1614	116628305	77.2	23	40.63	804
		Pfk (tetramer)	6-Phosphofructokinase — Pfk*°[c]	Stu0692	13629190	36.0	13	42.48	423
		Gapdh (tetramer)	Glyceraldehyde-3-phosphate dehydrogenase — Gapdh*°[c]	Stu1788	17066732	36.0	3	12.20	65
		PyrG (dimer)	CTP synthetase — PyrG	Stu0134	116627092	59.0	2	3.93	51
		RgpA/EpsF–EpsG–EpsI	Polysaccharide biosynthesis protein EpsF — RgpA/EpsF*°[c]	Stu1472	90655845	44.5	8	23.08	128
			Polysaccharide biosynthesis protein — EpsG[c]	–	24637480	42.8	5	15.45	88
			Polysaccharide biosynthesis protein — EpsI[c]	–	24637447	38.2	7	24.70	89
		Ldh (tetramer)	Lactate dehydrogenase — Ldh*°[c]	Stu1280	122267385	35.4	23	48.48	1209
		PtsH–PtsI	Phosphocarrier protein HPr — PtsH*[a]	Stu1265	55821270	8.9	3	58.62	6.18[d]
			Enzyme I — PtsI*°[a]	Stu1264	30027107	63.1	22	48.53	696
		Gla (tetramer)	Glycerol uptake facilitator protein — Gla[a]	Stu1671	55823574	30.8	2	9.41	78
U	96	Stu1225 (tetramer)	Oxidoreductase, short chain dehydrogenase/reductase — Stu1225*°	Stu1225	116627959	28.5	3	13.73	130
		ManL–PtsH	Mannose PTS system component IIAB — ManL*°[a]	Stu0333	30027111	35.8	19	68.18	995
			Phosphocarrier protein HPr — PtsH*[a]	Stu1265	55821270	8.9	3	54.02	101
		GroL–DnaK	60 kDa chaperonin — GroL*[c]	Stu0204	68566260	56.9	6	13.17	114
			Chaperon protein DnaK — DnaK*[c]	Stu0120	81676627	64.8	2	5.11	116
		PotA–RplB–RplD	Spermidine/putrescine import ATP-binding protein — PotA[a]	Stu1538	122267176	43.8	9	22.66	289
			50S ribosomal protein L2 — RplB*°	Stu1931	81820219	29.9	7	30.69	154
			50S ribosomal protein L4 — RplD*°	Stu1933	81558868	22.2	4	21.74	188
		CoaD (hexamer)	Phosphopantetheine adenylyltransferase — CoaD*°	Stu1648	116628337	18.7	5	52.12	286
		MurE–MurG–MurM	Mur ligase – MurE	Stu1254	55821261	49.4	9	25.95	331
			UDP-N-acetylglucosamine-N-acetylmuramyl-(pentapeptide) pyrophosphoryl-undecaprenol N-acetylglucosamine transferase — MurG*°[c]	Stu0732	81559554	40.1	6	16.85	201
			Peptidoglycan branched peptide synthesis protein, alanine adding enzyme — MurM[c]	Stu1155	13324647	46.2	9	28.71	312
		SecA–Tuf	Protein translocase subunit SecA — SecA*[a]	Stu1730	122266980	96.3	5	7.54	340
			Elongation factor Tu — Tuf*[c]	Stu0487	81559720	43.8	14	41.21	544
V	70	DapA–DapB	4-Hydroxy-tetrahydrodipicolinate synthase — DapA*	Stu1297	122267371	33.8	2	7.07	73

(continued on next page)

Table 1 (*continued*)

Band	Complex migration (kDa)	Protein complex	Protein name	Gene name	Accession	Mass (kDa)	Unique peptides	Sequence coverage (%)	Mascot score
			4-Hydroxy-tetrahydrodipicolinate reductase — DapB*	Stu0424	81559752	27.7	10	52.16	438
		MetN (dimer)	Methionine import ATP-binding protein — MetN[a]	Stu0301	81820355	38.7	8	23.10	235
		Pgma (tetramer)	2,3-Bisphosphoglycerate-dependent phosphoglycerate mutase — Pgma*[c]	Stu1204	81559295	26.2	26	74.78	782
		EpsD–EpsN–Ster1440	Polysaccharide biosynthesis protein — EpsD*[a]	Stu1109	24473738	27.5	4	22.22	108
			Polysaccharide biosynthesis protein — EpsN*°[c]	–	24637452	39.0	7	23.71	204
			Cell wall biosynthesis glycosyltransferase — Ster1440*[c]	Ster1440	116628179	27.1	4	21.43	143
		GltX–FabF	Glutamate-tRNA ligase — GltX[c]	Stu1814	67461637	55.3	2	4.34	42
			3-Oxoacyl-ACP synthase — FabF	Stu0388	116627299	43.5	4	13.17	189
		Tig–Pyk	Trigger factor — Tig	Stu0132	122268307	46.7	10	26.23	217
			Pyruvate kinase — Pyk*°[c]	Stu1196	161936368	54.5	7	18.40	229
		GlyS–RplB–RplM	Glycine-tRNA ligase beta subunit — GlyS	Stu0507	122268006	74.4	4	6.34	101
			50S ribosomal protein L2 — RplB	Stu1931	81820219	29.9	4	19.86	101
			50S ribosomal protein L13 — RplM	Stu0093	55822083	16.2	3	18.24	86
W	65	MurG–MurM	UDP-N-acetylglucosamine-N-acetylmuramyl-(pentapeptide) pyrophosphoryl-undecaprenol N-acetylglucosamine transferase — MurG*°[c]	Stu0732	122267800	40.2	3	11.52	91
			Peptidoglycan branched peptide synthesis protein, alanine adding enzyme — MurM[c]	Stu1155	13324647	46.2	15	40.10	549
		GlnQ–Peb1	Amino acid ABC transporter periplasmic protein — GlnQ*°[a,b]	Stu1162	116627888	30.9	4	15.16	103
			ABC-type polar amino acid transport system, ATPase component — Peb1*°[a]	Stu1161	116627887	28.1	12	44.71	491
		PlsX (dimer)	Phosphate acyltransferase — PlsX*°[c]	Stu0028	122268399	35.5	4	12.28	58
		RgpA/EpsF–EpsI	Polysaccharide biosynthesis protein EpsF — RgpA/EpsF°[c]	Stu1472	90655845	44.5	14	42.31	400
			Polysaccharide biosynthesis protein — EpsI[c]	–	24637447	38.2	11	26.52	386
		FabK (dimer)	Trans-2-enoyl-ACP reductase II — FabK*°	Stu0385	116627296	33.6	2	11.21	5.97[d]
		UspA (dimer)	Hypothetical protein — UspA*°[c]	Stu1637	55823541	16.9	8	56.00	217
		LivF–LivG	Branched chain amino acid ABC transporter ATP binding protein — LivF*[a]	Stu0363	55822340	25.5	2	14.83	68
			ABC-type branched-chain amino acid transport system, ATPase component — LivG*°[a]	Stu0362	116627277	27.9	4	14.57	92
		PhoU–PstB2	Phosphate uptake regulatory protein — PhoU*[c]	Stu1006	55737024	24.9	2	9.63	88
			ABC-type phosphate transport system, ATPase component — PstB2*[a]	Stu1005	116627797	28.0	3	16.67	144

Underlined are protein complex components for which interaction/oligomerization information was already available according to eNet and PSICQUIC analysis, literature data and/or crystallographic records present within the PDB database.

This table includes protein abbreviations used within the whole text.

[a] Refers to membrane proteins predicted by in silico analysis of the *Streptococcus thermophilus* genome [7].

[b] Refers to secretory proteins predicted by in silico analysis of the *Streptococcus thermophilus* genome [144].

[c] Refers to moonlighting proteins [72,73] or components whose transient localization on or close to the cell membrane has been already reported.

[d] Refers to protein identification data where Sequest results are shown; this condition occurred in the cases in which identification parameters were satisfied for Sequest but not for Mascot searching.

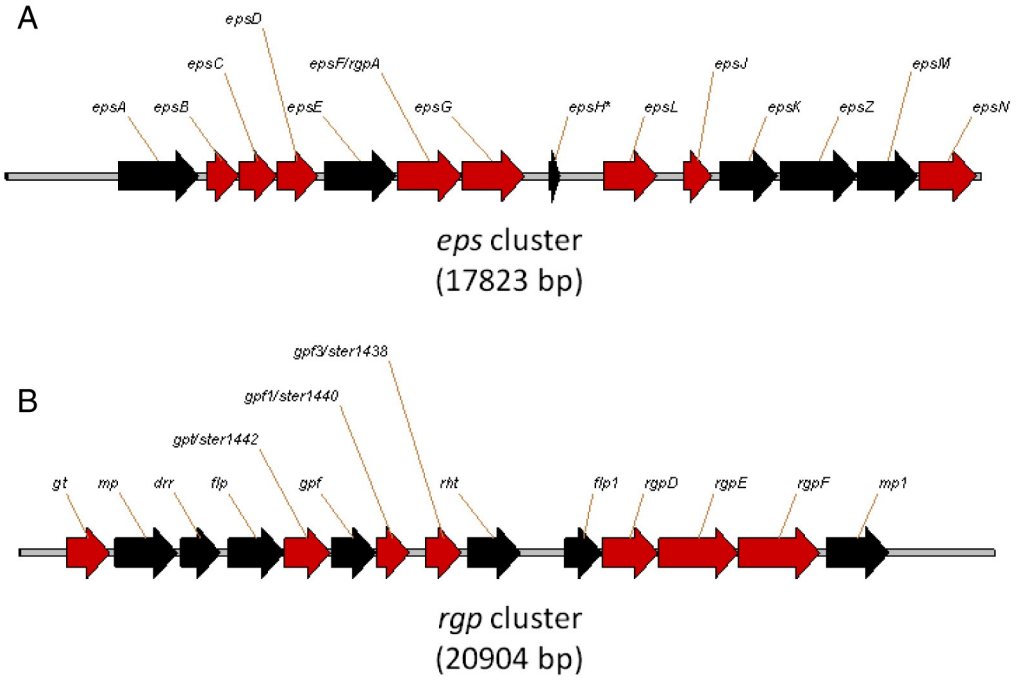

Fig. 3 – Schematic organization of the *eps* and *rgp* genes cluster in *Streptococcus thermophilus* DSM20617. Genes coding for proteins here identified in heteromultimeric and homomeric complexes are reported in red. Shown are genes and related product as deduced by BLAST analysis. Panel A. EPS cluster; *epsA*, cell envelope-related transcriptional attenuator; *epsB*, capsular polysaccharide biosynthesis protein; *epsC*, polysaccharide export protein, MPA1 family, G+ type; *epsD*, membrane-associated ATPase; *epsE*, galactosyl transferase; *epsF/rgpA*, rhamnosyl transferase; *epsG*, glycosyl transferase; *epsH, exopolysaccharide biosynthesis protein, truncated; *epsL*, β-glycosyltransferase; *epsJ*, glycosyltransferase; *epsK*, polysaccharide polymerase; *epsZ*, flippase, assisting in the membrane translocation of lipopolysaccharides; *epsM*, galactopyranose mutase; *epsN*, galactofuranose transferase. Asterisk indicates a truncated gene (*epsH*). Panel B. RGP cluster; *gt*, glucosyltransferase; *mp*, predicted membrane protein; *drr*, dTDP-4-dehydrorhamnose reductase; *flp*, flippase; *gtp/ster1442*, CDP-glycosylpolyol phosphate:glycosylpolyol glycosylpolyol phosphotransferase; *gpf*, β-1,3-glucosyltransferase; *gpf1/ster1440*, glycosyl transferase; *gpf3/ster1438*, glycosyl transferase; *rht*, α-D-GlcNAc-α-1,2-L-rhamnosyltransferase; *flp1*, rhamnose-containing polysaccharide translocation permease; *rgpD*, ABC transporter possibly involved in side chain formation of rhamnose-glucose polysaccharide; *rgpE*, glycosyltransferase possibly involved in side chain formation of rhamnose-glucose polysaccharide; *rgpF*, α-L-rha-α-1,3-L-rhamnosyltransferase; *mp1*, predicted membrane protein.**

the porter proteins, the permease LacS (essential for lactose uptake) was found as bound to the HtrA chaperone/protease involved in the folding/degradation of secreted proteins (Table 1). The crucial role of the secretory machinery for the proper localization of folded LacS within the cell membrane has been already reported [86,87]. A similar HtrA-bound condition was also observed for the phosphotransfer-driven group translocator ScrA, involved in sucrose transport. In both cases, our data suggest a specific function of HtrA in assisting the proper folding of these TMH-containing proteins and/or degradation of the corresponding misfolded counterparts. Molecular migration of both complexes in 1D-BN-PAGE was compatible with a dodecameric structure of HtrA containing a single substrate molecule, as already observed in other bacteria [88]. Conversely, native LacS and ScrA were absent within 1D-BN-PAGE, 2D-BN/urea-PAGE and 2D-BN/SDS-PAGE as homodimeric species [89,90] (Figs. 1, 2 and Table 1); this was not surprising on the basis of their recalcitrance to be extracted from membranes by soft detergents, as already observed in our laboratory [14].

Three complexes involving members of the phosphoenolpyruvate: glucose/mannose PTS [91], which play a key role in coupling active sugar transport across the cell membrane to a sequential phosphorylation cascade, were also detected by 1D-BN-PAGE. In particular, the mannose PTS system components IIAB (ManL) and IIC (ManM) were identified within a band migrating at about 196 kDa. Together with component IID (ManN), these proteins constitute the glucose/mannose PTS transporter with a 2:1:2 (ManL:ManM:ManN) stoichiometry [47,53,92]. Observed migration was consistent with an intact glucose/mannose PTS transporter. Its functional expression may be related to its regulatory functions more than in glucose transport, as already hypothesized [91]. On the other hand, ManL was also detected as bound to its phosphorylating effector PtsH (Fig. 1 and Table 1); measured gel migration was consistent with a dimeric state of both proteins therein, as already revealed by NMR analysis [93]. In parallel, PtsH was also observed to participate in another complex with PtsI (Fig. 1 and Table 1). Direct interaction of these expression products from two contiguous genes in the same ORF (stu1264 and stu1265) [91]

was already reported in *E. coli* [94]; also in this case, gel migration was in agreement with the presence of protein dimers within the complex [95]. Detection of ManL–PtsH and PtsH–PtsI complexes in 1D-BN-PAGE was very surprising based on their underlying, relatively weak protein interactions [93,95]. Their observation was putatively ascribed to the relative high concentration of its single constituents, namely ManL and PtsI, as revealed by 2D-BN/urea-PAGE, and the very reduced mass increase of the corresponding complexes due to PtsH contribution (ΔM ~ 9 kDa) (Fig. 1).

The archetypal member of the aquaporin superfamily, i.e. glycerol facilitator protein, was also detected in 1D-BN-PAGE and 2D-BN/urea-PAGE (Fig. 1). Its migration properties (at about 140 kDa) and the absence of known interactors of this porin in the corresponding gel portion, as deduced by eNet and PSICQUIC analysis, strongly supported the occurrence of this protein as tetrameric species, in agreement with previous cryoelectron microscopy and X-ray crystallography studies [96].

Within the ABC transporter group, a number of products from contiguous genes present within the same ORF were identified within distinct bands from 1D-BN-PAGE or as vertical lines of spots in 2D-BN/urea-PAGE and 2D-BN/SDS-PAGE (Figs. 1, 2 and Table 1). This was the case of the binary LmrA1(stu0433)–LmrA2(stu0434), stu0296–stu0297, stu0808–stu0809, Peb1(stu1161)–GlnQ(stu1162), LivG(stu0362)–LivF(stu0363) and PstB2(stu1005)–PhoU(stu1006) complexes; in the latter case, another complex (PstB2–PhoU–FtsZ–Tuf) was also recognized as made of additional cell cytoskeletal proteins. Specific ABC transporter components were also identified in additional macromolecular aggregates migrating in 1D-BN-PAGE at different mass values (Fig. 1 and Table 1). Only for Peb1–GlnQ, LivG–LivF, PstB2–PhoU and PstB2–PhoU–FtsZ–Tuf complexes, measured migration properties were in good agreement with what expected on the basis of the corresponding theoretical mass values. For the remaining complexes, additional constituents determining observed migration in 1D-BN-PAGE may have escaped a positive MS identification due to the low amount of protein generally detected, as already reported for other bacteria [44,45,52,55,57]. From their migration in 1D-BN-PAGE, 2D-BN/urea-PAGE and 2D-BN/SDS-PAGE, previous literature data and the organization of the corresponding ABC transporter gene clusters in *S. thermophilus*, it is tempting to speculate that components at 222 and 135 kDa correspond to intact stu0808–stu0809–stu0810–stu0811 and PstS–PstB1–PstB2–PstC1–PstC2–PhoU complexes, respectively [6,7,44,45,52,55,57]. While information on putative functional efficiency of LmrA1–LmrA2, Peb1–GlnQ, LivG–LivF, PstB2–PhoU and stu0808–stu0809 interactions may be deduced by simple genome analysis, being part of complete multidrug (drugE2) family ABC exporter and polar amino acid, branched-chain amino acid, phosphate and carbohydrate ABC uptake transporters, respectively [6,7,97,98], it is no clear whenever stu0296–stu0297 are a part of an active protein machinery, being constituents of an incomplete transporter [6,7].

We also observed the larger part of the respiratory chain-related F_1F_0-ATP synthase complex, which catalyzes ATP synthesis during oxidative phosphorylation and ATP hydrolysis to generate the transmembrane proton electrochemical gradient required for different cell functions [99]. F_1F_0-ATP synthase contains 8 different subunits in a known stoichiometry ($\alpha_3\beta_3\gamma\delta\varepsilon AB_2C_{10-14}$) and exhibits a total molecular mass of about 530 kDa; the complex consists of 2 parts designated as F_0 and F_1. F_0 is membrane embedded and consists of subunits A, B and C, while F_1 is membrane-extrinsic and consists of 5 subunits, i.e. α, β, γ, δ and ε [100]. In this study, we observed only the F_1 part, which was detected within 3 distinct bands in 1D-BN-PAGE or as vertical lines of spots in 2D-BN/urea-PAGE and 2D-BN/SDS-PAGE (Figs. 1, 2 and Table 1). The first one (at about 403 kDa) well fitted with the molecular mass of the whole F_1 complex and contained all its subunits. The second (at 371 kDa) and the third one (at 333 kDa) showed progressive disappearance of γ, or γ and ε subunits, respectively, which was associated with a partial F_1 complex decomposition. Our results were in good agreement with previous observations on other G+ and G– bacteria [40,43–47,52,53].

3.4. *Cell growth and morphology*

Bacterial division is generally driven through the formation of a macromolecular machinery (divisome) containing at least a dozen of proteins, which assembles with a defined dependence hierarchy at a specific cell membrane site [101]. The way in which

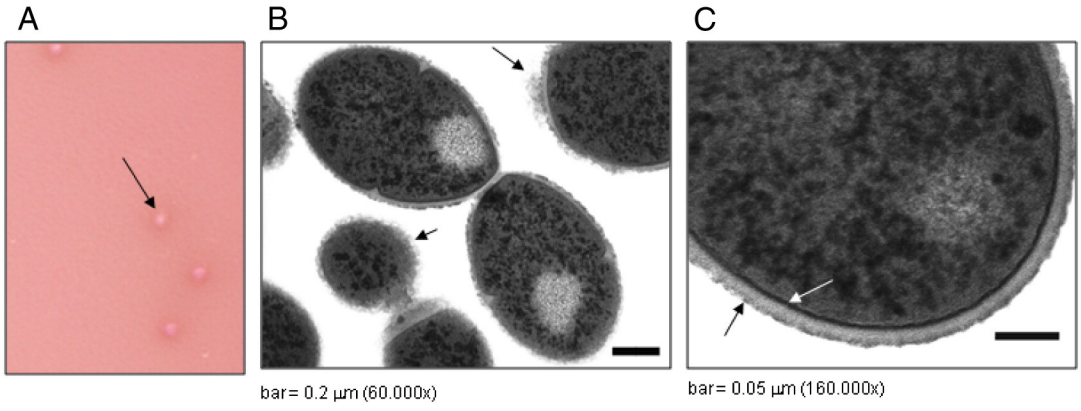

Fig. 4 – Microscopic analysis of *Streptococcus thermophilus* DSM20617. Panel A. White colonies for ropy *Streptococcus thermophilus* DSM20617 in ruthenium red milk agar plate. Panels B and C. Transmission electron micrographs showing *Streptococcus thermophilus* DSM20617 cells. The black arrows indicate the polysaccharide matrix present on the surface of bacterial cells. The white arrow indicates the bacterial cell wall.

the divisome assembles has been studied extensively in *E. coli* and *Bacillus subtilis*, leading to related assembly pathways that require the sequential assembly of different subcomplexes [102,103]. In fact, additional proteins associated with cell cytoskeletal structure and peptidoglycan (PG) biosynthesis transiently interact with the divisome machinery depending on division moment. Likewise other bacteria, various genes coding for division proteins in *S. thermophilus* occur within a specific ORF (stu0731–0740), where genes involved in cell wall biosynthesis are also present [6,7]. Additional genes coding for cell morphogenesis proteins and PG synthesis enzymes reside in distinct ORFs.

In our study, a number of macromolecular aggregates were identified in 1D-BN-PAGE and 2D-BN/urea-PAGE experiments. In particular, FtsZ–EzrA–DivIVA–MurG, FtsZ–DivIVA–MurG, FtsZ–EzrA–DivIVA, FtsZ–DivIVA, FtsZ–MurG–Pbp2X–SecA–Tuf, FtsZ–DivIVA–SecA–PrtM–Tuf, FtsZ–DivIVA–MurG–Pbp2X–Tuf, FtsZ–SecA–DivIVA–FtsY, MurG–MurM–MurE–Pbp2X, DivIVA–MurG–SecA, MurG–MurM–MurE–Upps, MurG–MurM–MurE and MurG–MurM complexes were characterized, in agreement with previous interaction studies (as also verified by eNet and PSICQUIC analysis) [34,40,47,104]. Considering the possible occurrence of oligomeric proteins (for FtsZ, DivIVA and SecA) within observed complexes, measured migration properties were in good agreement with what expected on the basis of the corresponding theoretical mass values. Ascertained assemblies often reflected progressive decomposition of higher structures. In general, complex composition highlighted the simultaneous occurrence of entries uniquely made of elements from the divisome machinery, of enzymes involved in PG biosynthesis, or where mixed elements from both protein classes occurred together. In this context, it has been already suggested that, after initial division stages driven by FtsZ ring formation [105], the divisome locally recruits an assembled multiprotein Mur subcomplex made of enzymes assisting lateral envelope growth [101,102,106]. PG glycosyltransferase MurG was suggested to be a common component of both complexes playing a crucial role for their interaction [107]. Our results were consistent with this scenario. In rod-shaped cells, it has been hypothesized that the cotranslational assembly and localization of the divisome and of the Mur subcomplex, driving the flux of PG precursors toward the septum synthesis machinery, occur through a genomic channeling mechanism [101].

Ascertained FtsZ–MurG–Pbp2X–SecA-Tuf, FtsZ–DivIVA–SecA–PrtM–Tuf, FtsZ–SecA–DivIVA–FtsY and DivIVA–MurG–SecA complexes also included proteins of the secretory machinery [86,87], namely SecA, FtsY and PrtM. Inclusion of the motor ATPase SecA has been already reported in cell wall biosynthesis and division functional modules of other bacteria [104]; it has been related to the possible role of this protein in directing secretion of the PG synthetic apparatus to regions where PG biosynthesis occur [108]. In fact, many proteins that carry out or mediate PG biosynthesis contains TMHs or membrane anchors linked to large extracellular domains, which are likely exported in a SecA-dependent manner. Bioinformatic analysis of our data confirmed the capability of SecA to interact with FtsZ and MurG [104], thus sanctioning a putative cross-talk of the bacterial secretory machinery with the cell growth- and morphology-affecting complexes mentioned above.

3.5. *Protein elongation, secretion and folding*

According to *S. thermophilus* genome analysis, components of the secretory machinery include signal recognition particle proteins Ffh and FtsY, trigger factor chaperone RopA, Sec translocase constituents (SecA–SecYEG and YajC), two ortholog proteins of YidC (stu1810 and stu0245) interacting with the translocase, TatA and TatC components of the twin Arg translocation pathway, various signal peptidases (SipA, SipB, LspA, Lgt, Sip and PilD), a PrsA/PrtM peptidylprolyl isomerase (lipoprotein) assisting the folding of the exported proteins and HtrA [7].

In addition to the already-mentioned complexes containing elements from different functional modules, protein assemblies uniquely related to the secretory machinery [86,87] were also recognized on the *S. thermophilus* membrane. In particular, SecA–FtsY–PrtM, SecA–FtsY–Ffh and SecA–Tuf complexes were identified in 1D-BN-PAGE and 2D-BN/urea-PAGE experiments (Table 1). These results were in good agreement with previous studies on other bacteria where, similarly to what reported here, additional complexes (Ffh–FusA–Tuf, Tuf–GroL–ClpL–PotA, Tuf–RpsA–FusA–DnaK, DnaK–RpsA–ClpL, DnaK–RpsA–Pyk, RpsA–ClpL, GroL–DnaK and Tig–Pyk) related to the elongation cycle of protein biosynthesis and/or involving protein folding-assisting interactions with various chaperones were also observed [32–34,46,50,53,104,109–111]. Ascertained relationships were coherent with that observed following eNet and PSICQUIC analysis. At present, it is not clear if these complexes were related to nascent, unfolded polypeptide chains before their localization close to/within the lipid bilayer or to membrane proteins that are partially unfolded therein. A number of chaperones, elongation factors and ribosomal protein antigens with moonlighting properties were identified as complex constituents, in agreement with previous investigations [72,73,112–115]. Among that, 60 kDa chaperonin GroL that was identified as an abundant homomeric complex migrating at about 518 kDa in 1D-BN-PAGE; its migration properties were not coherent with the characteristic epta- or tetradecameric structure of this chaperone, but strongly resembled those already observed during 2D-BN/SDS-PAGE analysis of membrane proteins from *H. pylori* [50]. In vitro studies have demonstrated that GroEL can mediate post-translational membrane insertion of lactose permease [116], bacteriorhodopsin [117] and holin [118]. However, in a proteome wide screen no membrane proteins were identified as GroEL substrates [119]. An analogous homomeric condition was observed for the ATPase/protein unfoldase ClpL, which was also observed as a tetrameric species migrating in 1D-BN-PAGE at about 303 kDa, in agreement with previous analytical ultracentrifugation and light scattering experiments [120]. On the basis of what reported above, further studies have to be accomplished to unveil the precise structure–function relationship of these moonlighting chaperones in a membrane environment and their role in mediating inter-cellular interactions [72].

3.6. *Moonlighting proteins with different function*

In addition to the already-mentioned chaperones and elongation factors, other moonlighting proteins (GlnA, Eno, GdhA, RpoC, DeoD, Ldh, GapN, Pyk, Pfk, Gapdh, TpiA, Pgi, Pgma and GltX) were also identified as abundant component present on the membrane fraction of *S. thermophilus*; their peculiar localization

has been already reported in other bacteria, including streptococci and lactobacilli [42,72,73,113,114,121]. About half of them participate in the glycolytic pathway, but have also been reported to mediate adhesion to exogenous plasminogen, fibrinogen and cytoskeletal components as well as to modulate cell signaling processes [72]. Most of these moonlighting proteins occurred as homomeric complexes; this was the case of GlnA, Eno, GdhA, DeoD, GapN, Pyk, Pfk, Gapdh, Ldh and Pgma, which migrated in 1D-BN-PAGE as dodecameric, octameric, hexameric, hexameric, tetrameric, tetrameric, tetrameric, tetrameric, tetrameric and tetrameric species, respectively, in agreement with previous proteomic studies on other bacteria [42,48,53] and protein structures present within the PDB database (http://www.rcsb.org/pdb/home/home.do). These findings suggest the maintenance of the corresponding protein quaternary structures also in a membrane environment.

On the other hand, known moonlighting proteins were also observed to participate in heteromeric complexes, as in the case of the RpoC, which was present in the complexes RpoA–RpoB–RpoC, RpoB–RpoC–stu0256 and RpoC–RplJ–RplS. The occurrence of the RNA polymerase in bacterial membrane is not surprising [53,114]; a band showing a migration compatible with the whole biosynthetic machinery (where only RpoA, RpoB and RpoC were identified) has been already reported in *E. coli* [53]. In this case and in the current study, remaining RNA polymerase constituents may have escaped MS identification due to the low amount of protein present. RpoB and RpoC were also observed in other complexes; in this context, BLAST analysis identified stu0256 as a putative nucleotide triphosphate pyrophosphatase that hydrolyzes non-standard purines preventing their incorporation into RNA. Analogously, participation into heteromeric complexes was also verified for moonlighting dimeric proteins TpiA and Pgi that, according to their migration in 1D-BN-PAGE, were involved in binding to dimeric Pfl and MetN, respectively. These interaction data were in agreement with previous observations in *E. coli* [32]. Also in these cases, predicted protein oligomerization in a membrane environment was similar to that observed in aqueous media. Finally, moonlighting protein GltX was observed as bound to FabF and as monomeric species (data not shown), in agreement with previous chromatographic data [122]. This protein was previously identified as a cell wall-associated antigen in *S. pneumoniae* [121].

Other proteins generally reported as cytosolic components were also observed in the membrane fraction of *S. thermophilus*; they included Dpr, Prs1, Prs2, PurB, PlsX and UspA (Figs. 1 and 2). A careful evaluation of available literature confirmed their possible occurrence also on bacterial membrane. This was the case of the peroxide-resistance protein Dpr, which was detected on the membrane of *H. pylori* and *E. coli* grown under various environmental conditions [50,123,124]. This protein was suggested to have a scavenging function against reactive oxygen species and Fe ion misbalance as well as a protective role against DNA damage [125]. Recently, it was proved to influence the attachment of bacteria to abiotic surfaces [126]. Its migration in 1D-BN-PAGE was consistent with a dodecameric structure [125], whose high stability was also appreciated after urea-PAGE (Fig. 1) and SDS-PAGE (Fig. 1), as already observed in *C. thermocellum* [45]. On the other hand, two phosphoribosylpyrophosphate synthase isoforms, namely Prs1 and Prs2, were observed to migrate as a vertical line of spots in 2D-BN/SDS-PAGE (Fig. 2 and Table 1). Homologue proteins from other bacteria have a functional hexameric structure [127,128]; this information, together with our PSICQUIC analysis that suggested a direct interaction between Prs1 and Prs2, was fully compatible with a heteromeric complex migrating at about 464 kDa, as revealed by 1D-BN-PAGE analysis. Phosphoribosylpyrophosphate synthase was observed as a membrane-bound component in human and rat cells [129,130]. In bacteria, its function has been associated to the biosynthesis of phosphoribosyl-1-pyrophosphate, a central metabolite precursor for cell wall sugar components [131]. Other membrane-associated proteins mentioned above occurred as homomeric complexes. In agreement with data present within the PDB database (http://www.rcsb.org/pdb/home/home.do), PurB, UspA and PlsX migrated in 1D-BN-PAGE as tetrameric, dimeric and dimeric species (Table 1), respectively, thus confirming the maintenance of their protein quaternary structures also in a membrane environment. PlsX was also observed to form a heteromeric complex with LysS and SerS, coherently with data deduced from eNet and PSICQUIC analysis. The occurrence of PurB, PlsX and UspA on the bacterial membrane has been already reported [53,132] and associated with the biosynthesis of fatty acids and membrane phospholipids [133] or with the bacterial response to environmental stresses [134], respectively.

3.7. *Proteolytic enzymes and other proteins*

Membrane proteases detected in this study included FtsH, PepC and PepB, which migrated in 1D-BN-PAGE as homomeric species present at about 430, 288 and 131 kDa, respectively. In the first case, observed migration was consistent with the ascertained hexameric crystallographic structure of this membrane-spanning ATP-dependent metalloprotease [135]. It plays a key role in quality and regulatory control within the cell by degrading a unique subset of substrates. In fact, FtsH is able to identify and degrade nonfunctional or damaged membrane proteins by pulling them out of the lipid bilayer, followed by further substrate unfolding and translocation into the proteolytic chamber [111]. On the other hand, PepC is an endopeptidase with moonlighting properties that were observed among the antigenic cell wall-associated proteins of *S. pneumoniae*, eliciting protective immune response in the mouse [121]. Also in this case, 1D-BN-PAGE results were in agreement with the protein hexameric quaternary structure reported in the PDB database. Finally, PepB was never reported as a membrane component so far; its electrophoretic migration was consistent with a dimeric crystallographic structure [136].

Analogous considerations on the absence of data concerning protein membrane localization were valid for phosphopantetheine adenyltransferase CoaD, hypothetical protein stu1225 (homologous to short-chain dehydrogenase/reductases), acetolactate synthase Als, CTP synthase PyrG and enoyl–acyl carrier protein reductase FabK. These proteins were observed to migrate in 1D-BN-PAGE as hexameric, tetrameric, tetrameric, dimeric and dimeric species, respectively, in agreement with available data on their quaternary structure [137–141].

4. Conclusions

Although milk is a rich growth medium for many microorganisms, bacteria that grow and compete well in the milk environment must, at minimum, be able to use lactose as an energy source and milk proteins as a source of amino acids. The adaptation of *S. thermophilus* to the milk environment is reflected by several observations at genomic and transcriptome levels [6–11,142,143], including the detection of specialized systems for metabolizing lactose, the general absence of other carbohydrate metabolic systems, the presence of amino acid and peptide scavenging machinery, and numerous stress response and host defense mechanisms.

In the present study, a combined approach based on 1D-BN-PAGE, 2D-BN/urea-PAGE, 2D-BN/SDS-PAGE and nLC–ESI-LIT-MS/MS was used to investigate membrane protein complexes in *S. thermophilus* cells at their early exponential phase. We were able to reproducibly separate individual proteins and to reveal protein–protein interactions, consistently with the results obtained through independent, traditional biochemical and biophysical procedures. Among the 110 non-redundant components present in the heteromeric/homomeric complexes reported here, 31 corresponded to about 10% of the 326 membrane proteins predicted by in silico analysis of the *S. thermophilus* genome [7], while 7 matched about 7% of the 98 secretory proteins analogously envisaged [144]; on the other hand, 44 species were identified as moonlighting proteins [42,72,73] or components whose transient localization on or close to the bacterial membrane have been already reported. Thus, membrane protein machineries involved in essential biochemical processes, such as polysaccharide biosynthesis, molecular uptake, energy metabolism, cell division, protein secretion and folding, were characterized for their constitutive elements. Information on hypothetical proteins was also derived. In general, most (about 84%) of the heteromeric/homomeric complexes reported in this study were coherent with that already described in other bacteria, as verified by eNet and PSICQUIC analysis of the corresponding hortolog species or by evaluation of literature data and crystallographic information present within the PDB database. Novel information on protein machineries involved in exopolysaccharide and peptidoglycan biosyntheses, cell division and protein secretion were obtained. The approach reported here paves the way for a further functional characterization of these protein complexes and will facilitate future studies of their assembly and composition during various experimental conditions and in different mutant backgrounds, with important consequences for biotechnological applications of this bacterium in dairy productions.

Supplementary data to this article can be found online at http://dx.doi.org/10.1016/j.jprot.2013.09.007.

Acknowledgments

This work was partially supported by funds from: i) the Italian Ministry of Economy and Finance to CNR for the project "Innovazione e sviluppo del Mezzogiorno — Conoscenze Integrate per Sostenibilità ed Innovazione del Made in Italy Agroalimentare" — Legge n. 191/2009; and ii) Regione Campania for the Rete di Spettrometria di Massa della Campania (RESMAC) and for the Project QUARC — Qualità delle produzioni tipiche campane ed il suo territorio: approcci innovativi ed integrati per rafforzare la competitività del sistema Agroalimentare (A.G.C.6 - settore 1), bando CAMPUS.

REFERENCES

[1] Fox PF. Cheese: chemistry, physics and microbiology. London UK: Chapman & Hall; 1993.
[2] Leroy F, De Vuyst L. Lactic acid bacteria as functional starter cultures for the food fermentation industry. Trends Food Sci Technol 2004;15:67–78.
[3] Tamime AY, Deeth HC. Yogurt: technology and biochemistry. J Food Protect 1980;43:939–77.
[4] Mitchell TJ. The pathogenesis of streptococcal infections: from tooth decay to meningitis. Nat Rev Microbiol 2003;1:219–30.
[5] Tettelin H. Streptococcal genomes provide food for thought. Nat Biotechnol 2004;22:1523–4.
[6] Bolotin A, Quinquis B, Renault P, Sorokin A, Ehrlich SD, Kulakauskas S, et al. Complete sequence and comparative genome analysis of the dairy bacterium *Streptococcus thermophilus*. Nat Biotechnol 2004;22:1554–8.
[7] Hols P, Hancy F, Fontaine L, Grossiord B, Prozzi D, Leblond-Bourget N, et al. New insights in the molecular biology and physiology of *Streptococcus thermophilus* revealed by comparative genomics. FEMS Microbiol Rev 2005;29:435–63.
[8] Goh YJ, Goin C, O'Flaherty S, Altermann E, Hutkins R. Specialized adaptation of a lactic acid bacterium to the milk environment: the comparative genomics of *Streptococcus thermophilus* LMD-9. Microb Cell Fact 2011;10(Suppl. 1):S22.
[9] Delorme C, Bartholini C, Luraschi M, Pons N, Loux V, Almeida M, et al. Complete genome sequence of the pigmented *Streptococcus thermophilus* strain JIM8232. J Bacteriol 2011;193:5581–2.
[10] Kang X, Ling N, Sun G, Zhou Q, Zhang L, Sheng Q. Complete genome sequence of *Streptococcus thermophilus* strain MN-ZLW-002. J Bacteriol 2012;194:4428–9.
[11] Sun Z, Chen X, Wang J, Zhao W, Shao Y, Wu L, et al. Complete genome sequence of *Streptococcus thermophilus* strain ND03. J Bacteriol 2011;193:793–4.
[12] Mora D, Monnet C, Daffonchio D. Balancing the loss and the acquisition of pathogenic traits in food-associated bacteria. Microbiology 2005;151:3814–6.
[13] Arena S, D'Ambrosio C, Renzone G, Rullo R, Ledda L, Vitale F, et al. A study of *Streptococcus thermophilus* proteome by integrated analytical procedures and differential expression investigations. Proteomics 2006;6:181–92.
[14] Salzano AM, Arena S, Renzone G, D'Ambrosio C, Rullo R, Bruschi M, et al. A widespread picture of the *Streptococcus thermophilus* proteome by cell lysate fractionation and gel-based/gel-free approaches. Proteomics 2007;7:1420–33.
[15] Arioli S, Roncada P, Salzano AM, Deriu F, Corona S, Guglielmetti S, et al. The relevance of carbon dioxide metabolism in *Streptococcus thermophilus*. Microbiology 2009;155:1953–65.
[16] Dyer MD, Neff C, Dufford M, Rivera CG, Shattuck D, Bassaganya-Riera J, et al. The human-bacterial pathogen protein interaction networks of *Bacillus anthracis*, *Francisella tularensis*, and *Yersinia pestis*. PLoS One 2010;5:e12089.

[17] Hoebeke M, Chiapello H, Noirot P, Bessières P. SPiD: a subtilis protein interaction database. Bioinformatics 2001;17:1209–12.
[18] Shimoda Y, Shinpo S, Kohara M, Nakamura Y, Tabata S, Sato S. A large scale analysis of protein–protein interactions in the nitrogen-fixing bacterium *Mesorhizobium loti*. DNA Res 2008;15:13–23.
[19] Sato S, Shimoda Y, Muraki A, Kohara M, Nakamura Y, Tabata S. A large-scale protein–protein interaction analysis in *Synechocystis* sp. PCC6803. DNA Res 2007;14:207–16.
[20] Rain JC, Selig L, De Reuse H, Battaglia V, Reverdy C, Simon S, et al. The protein–protein interaction map of *Helicobacter pylori*. Nature 2001;409:211–5.
[21] Parrish JR, Yu J, Liu G, Hines JA, Chan JE, Mangiola BA, et al. A proteome-wide protein interaction map for *Campylobacter jejuni*. Genome Biol 2007;8:R130.
[22] Dove SL, Hochschild A. A bacterial two-hybrid system based on transcription activation. Methods Mol Biol 2004;261:231–46.
[23] Yang H, Tan Y, Zhang T, Tang L, Wang J, Ke Y, et al. Identification of novel protein–protein interactions of *Yersinia pestis* type III secretion system by yeast two hybrid system. PLoS One 2013;8:e54121.
[24] Hynes SO, McGuire J, Wadstrom T. Potential for proteomic profiling of *Helicobacter pylori* and other *Helicobacter* spp. using a ProteinChip array. FEMS Immunol Med Microbiol 2003;36:151–8.
[25] Gerber D, Maerkl SJ, Quake SR. An *in vitro* microfluidic approach to generating protein-interaction networks. Nat Methods 2009;6:71–4.
[26] Galeotti CL, Bove E, Pezzicoli A, Nogarotto R, Norais N, Pileri S, et al. Surface interactome in *Streptococcus pyogenes*. Mol Cell Proteomics 2012;11:M111015206.
[27] Menon AL, Poole II FL, Cvetkovic A, Trauger SA, Kalisiak E, Scott JW, et al. Novel multiprotein complexes identified in the hyperthermophilic archaeon *Pyrococcus furiosus* by non-denaturing fractionation of the native proteome. Mol Cell Proteomics 2009;8:735–51.
[28] Wodak SJ, Pu S, Vlasblom J, Séraphin B. Challenges and rewards of interaction proteomics. Mol Cell Proteomics 2009;8:3–18.
[29] Wittig I, Schägger H. Native electrophoretic techniques to identify protein–protein interactions. Proteomics 2009;9:5214–23.
[30] Enright AJ, Iliopoulos I, Kyrpides NC, Ouzounis CA. Protein interaction maps for complete genomes based on gene fusion events. Nature 1999;402:86–90.
[31] Ito T, Tashiro K, Kuhara T. Systematic analysis of *Saccharomyces cerevisiae* genome: gene network and protein–protein interaction network. Tanpakushitsu Kakusan Koso 2001;46:2407–13.
[32] Butland G, Peregrín-Alvarez JM, Li J, Yang W, Yang X, Canadien V, et al. Interaction network containing conserved and essential protein complexes in *Escherichia coli*. Nature 2005;433:531–7.
[33] Arifuzzaman M, Maeda M, Itoh A, Nishikata K, Takita C, Saito R, et al. Large-scale identification of protein–protein interaction of *Escherichia coli* K-12. Genome Res 2006;16:686–91.
[34] Hu P, Janga SC, Babu M, Díaz-Mejía JJ, Butland G, Yang W, et al. Global functional atlas of *Escherichia coli* encompassing previously uncharacterized proteins. PLoS Biol 2009;7:e96.
[35] Babu M, Kagan O, Guo H, Greenblatt J, Emili A. Identification of protein complexes in *Escherichia coli* using sequential peptide affinity purification in combination with tandem mass spectrometry. J Vis Exp 2012;69:e4057.
[36] Kühner S, van Noort V, Betts MJ, Leo-Macias A, Batisse C, Rode M, et al. Proteome organization in a genome-reduced bacterium. Science 2009;326:1235–40.
[37] Cherkasov A, Hsing M, Zoraghi R, Foster LJ, See RH, Stoynov N, et al. Mapping the protein interaction network in methicillin-resistant *Staphylococcus aureus*. J Proteome Res 2011;10:1139–50.
[38] Pelletier DA, Hurst GB, Foote LJ, Lankford PK, McKeown CK, Lu TY, et al. A general system for studying protein–protein interactions in Gram-negative bacteria. J Proteome Res 2008;7:3319–28.
[39] Wittig I, Schägger H. Features and applications of blue-native and clear-native electrophoresis. Proteomics 2008;8:3974–90.
[40] Dresler J, Klimentova J, Stulik J. Bacterial protein complexes investigation using blue native PAGE. Microbiol Res 2011;166:47–62.
[41] Wessels HJ, Vogel RO, van den Heuvel L, Smeitink JA, Rodenburg RJ, Nijtmans LG, et al. LC–MS/MS as a alternative for SDS-PAGE in blue native analysis of protein complexes. Proteomics 2009;9:4221–8.
[42] Marzoa J, Sánchez S, Ferreirós CM, Criado MT. Identification of *Neisseria meningitidis* outer membrane vesicle complexes using 2-D high resolution clear native/SDS-PAGE. J Proteome Res 2010;9:611–9.
[43] D'Amici GM, Rinalducci S, Murgiano L, Italiano F, Zolla L. Oligomeric characterization of the photosynthetic apparatus of *Rhodobacter sphaeroides* R261 by nondenaturing electrophoresis methods. J Proteome Res 2010;9:192–203.
[44] Dresler J, Klimentova J, Stulik J. *Francisella tularensis* membrane complexome by blue native/SDS-PAGE. J Proteomics 2011;751:257–69.
[45] Peng Y, Luo Y, Yu T, Xu X, Fan K, Zhao Y, et al. A blue native-PAGE analysis of membrane protein complexes in *Clostridium thermocellum*. BMC Microbiol 2011;11:22.
[46] Zheng J, Wei C, Zhao L, Liu L, Leng W, Li W, et al. Combining blue native polyacrylamide gel electrophoresis with liquid chromatography tandem mass spectrometry as an effective strategy for analyzing potential membrane protein complexes of *Mycobacterium bovis bacillus* Calmette–Guérin. BMC Genomics 2011;18:12–40.
[47] Maddalo G, Chovanec P, Stenberg-Bruzell F, Nielsen HV, Jensen-Seaman MI, Ilag LL, et al. A reference map of the membrane proteome of *Enterococcus faecalis*. Proteomics 2011;11:3935–41.
[48] Wang ZJ, Xu XP, Fan KQ, Jia CJ, Yang KQ. Sample preparation for two-dimensional blue native/SDS polyacrylamide gel electrophoresis in the identification of *Streptomyces coelicolor* cytoplasmic protein complexes. J Biochem Biophys Methods 2007;10(70):565–72.
[49] Tsirogianni E, Aivaliotis M, Papasotiriou DG, Karas M, Tsiotis G. Identification of inducible protein complexes in the phenol degrader *Pseudomonas* sp. strain phDV1 by blue native gel electrophoresis and mass spectrometry. Amino Acids 2006;30:63–72.
[50] Bernarde C, Lehours P, Lasserre JP, Castroviejo M, Bonneu M, Mégraud F, et al. Complexomics study of two *Helicobacter pylori* strains of two pathological origins: potential targets for vaccine development and new insight in bacteria metabolism. Mol Cell Proteomics 2010;9:2796–826.
[51] Pyndiah S, Lasserre JP, Ménard A, Claverol S, Prouzet-Mauléon V, Mégraud F, et al. Two-dimensional blue native/SDS gel electrophoresis of multiprotein complexes from *Helicobacter pylori*. Mol Cell Proteomics 2007;6:193–206.
[52] Stenberg F, Chovanec P, Maslen SL, Robinson CV, Ilag LL, von Heijne G, et al. Protein complexes of the *Escherichia coli* cell envelope. J Biol Chem 2005;280:34409–19.
[53] Lasserre JP, Beyne E, Pyndiah S, Lapaillerie D, Claverol S, Bonneu M. A complexomic study of *Escherichia coli* using two-dimensional blue native/SDS polyacrylamide gel electrophoresis. Electrophoresis 2006;27:3306–21.

[54] Aivaliotis M, Karas M, Tsiotis G. High throughput two-dimensional blue-native electrophoresis: a tool for functional proteomics of cytoplasmatic protein complexes from *Chlorobium tepidum*. Photosynth Res 2006;88:143–57.
[55] Aivaliotis M, Karas M, Tsiotis G. An alternative strategy for the membrane proteome analysis of the green sulfur bacterium *Chlorobium tepidum* using blue native PAGE and 2-D PAGE on purified membranes. J Proteome Res 2007;6:1048–58.
[56] Farhoud MH, Wessels HJ, Steenbakkers PJ, Mattijssen S, Wevers RA, van Engelen BG, et al. Protein complexes in the archaeon *Methanothermobacter thermautotrophicus* analyzed by blue native/SDS-PAGE and mass spectrometry. Mol Cell Proteomics 2005;4:1653–63.
[57] Goll J, Rajagopala SV, Shiau SC, Wu H, Lamb BT, Uetz P. MPIDB: the microbial protein interaction database. Bioinformatics 2008;24:1743–4.
[58] Franceschini A, Szklarczyk D, Frankild S, Kuhn M, Simonovic M, Roth A, et al. STRING v91: protein–protein interaction networks, with increased coverage and integration. Nucleic Acids Res 2013;41:D808–15.
[59] Kerrien S, Aranda B, Breuza L, Bridge A, Broackes-Carter F, Chen C, et al. The IntAct molecular interaction database in 2012. Nucleic Acids Res 2012;40:D841–6.
[60] Salwinski L, Miller CS, Smith AJ, Pettit FK, Bowie JU, Eisenberg D. The database of interacting proteins: 2004 update. Nucleic Acids Res 2004;32:D449–51.
[61] Chatr-Aryamontri A, Breitkreutz BJ, Heinicke S, Boucher L, Winter A, Stark C, et al. The BioGRID interaction database: 2013 update. Nucleic Acids Res 2013;41:D816–23.
[62] Aranda B, Blankenburg H, Kerrien S, Brinkman FS, Ceol A, Chautard E, et al. PSICQUIC and PSISCORE: accessing and scoring molecular interactions. Nat Methods 2011;8:528–9.
[63] Schagger H, von Jagow G. Blue native electrophoresis for isolation of membrane protein complexes in enzymatically active form. Anal Biochem 1991;199:223–31.
[64] Candiano G, Bruschi M, Musante L, Santucci L, Ghiggeri GM, Carnemolla B, et al. Blue silver: a very sensitive colloidal Coomassie G-250 staining for proteome analysis. Electrophoresis 2004;25:1327–33.
[65] Talamo F, D'Ambrosio C, Arena S, Del Vecchio P, Ledda L, Zehender G, et al. Proteins from bovine tissues and biological fluids: defining a reference electrophoresis map for liver, kidney, muscle, plasma and red blood cells. Proteomics 2003;3:440–60.
[66] Scippa GS, Rocco M, Ialicicco M, Trupiano D, Viscosi V, Di Michele M, et al. The proteome of lentil (*Lens culinaris* Medik) seeds: discriminating between landraces. Electrophoresis 2010;31:497–506.
[67] Aziz RK, Bartels D, Best AA, DeJongh M, Disz T, Edwards RA, et al. The RAST server: rapid annotations using subsystems technology. BMC Genomics 2008;9:75.
[68] Altschul SF, Gish W, Miller W, Myers EW, Lipman DJ. Basic local alignment search tool. J Mol Biol 1990;215:403–10.
[69] Mora D, Fortina MG, Parini C, Ricci G, Gatti M, Giraffa G, et al. Genetic diversity and technological properties of *Streptococcus thermophilus* strains isolated from dairy products. J Appl Microbiol 2002;93:278–87.
[70] Stingele F, Neeser JR, Mollet B. Identification and characterization of the eps (exopolysaccharide) gene cluster from *Streptococcus thermophilus* Sfi6. J Bacteriol 1996;178:1680–90.
[71] Fandiño AS, Rais I, Vollmer M, Elgass H, Schägger H, Karas M. LC–nanospray-MS/MS analysis of hydrophobic proteins from membrane protein complexes isolated by blue-native electrophoresis. J Mass Spectrom 2005;40:1223–31.
[72] Henderson B, Martin A. Bacterial moonlighting proteins and bacterial virulence. Curr Top Microbiol Immunol 2013;358:155–213.
[73] Kainulainen V. Moonlighting proteins of *Lactobacillus crispatus*: extracellular localization, cell wall anchoring and interactions with the host. [PhD Thesis] Helsinki University; 2012 1–80.
[74] Senini L, Ricci G, Manachini PL, Mora D. EPS phenotype and genotype in *Streptococcus thermophilus* strains of dairy origin. Ann Microbiol 2004;54:59–71.
[75] Laws A, Gu Y, Marshall V. Biosynthesis, characterisation, and design of bacterial exopolysaccharides from lactic acid bacteria. Biotechnol Adv 2001;19:597–625.
[76] Yother J. Capsules of *Streptococcus pneumoniae* and other bacteria: paradigms for polysaccharide biosynthesis and regulation. Annu Rev Microbiol 2011;65:563–81.
[77] De Vuyst L, Weckx S, Ravyts F, Herman L, Leroy F. New insights into the exopolysaccharide production of *Streptococcus thermophilus*. Int Dairy J 2011;21:586–91.
[78] Rasmussen TB, Danielsen M, Valina O, Garrigues C, Johansen E, Pedersen MB. *Streptococcus thermophilus* core genome: comparative genome hybridization study of 47 strains. Appl Environ Microbiol 2008;74:4703–10.
[79] Chapot-Chartier MP, Vinogradov E, Sadovskaya I, Andre G, Mistou MY, Trie-Cout P, et al. Cell surface of *Lactococcus lactis* is covered by a protective polysaccharide pellicle. J Biol Chem 2010;285:10464–71.
[80] Bender MH, Yother J. CpsB is a modulator of capsule-associated tyrosine kinase activity in *Streptococcus pneumonia*. J Biol Chem 2001;276:47966–74.
[81] Henriques MX, Rodrigues T, Carido M, Ferreira L, Filipe SR. Synthesis of capsular polysaccharide at the division septum of *Streptococcus pneumoniae* is dependent on a bacterial tyrosine kinase. Mol Microbiol 2011;82:515–34.
[82] Cefalo AD, Broadbent JR, Welker DL. Protein–protein interactions among the components of the biosynthetic machinery responsible for exopolysaccharide production in *Streptococcus thermophilus* MR-1C. J Appl Microbiol 2011;10:801–12.
[83] Minic Z, Marie C, Delorme C, Faurie JM, Mercier G, Ehrlich D, et al. Control of EpsE, the phosphoglycosyltransferase initiating exopolysaccharide synthesis in *Streptococcus thermophilus*, by EpsD tyrosine kinase. J Bacteriol 2007;189:1351–7.
[84] Péant B, LaPointe G, Gilbert C, Atlan D, Ward P, Roy D. Comparative analysis of the exopolysaccharide biosynthesis gene clusters from four strains of *Lactobacillus rhamnosus*. Microbiology 2005;151:1839–51.
[85] Lebeer S, Verhoeven TL, Francius G, Schoofs G, Lambrichts I, Dufrêne Y, et al. Identification of a gene cluster for the biosynthesis of a long, galactose-rich exopolysaccharide in *Lactobacillus rhamnosus* GG and functional analysis of the priming glycosyltransferase. Appl Environ Microbiol 2009;75:3554–63.
[86] Dalbey RE, Wang P, Kuhn A. Assembly of bacterial inner membrane proteins. Annu Rev Biochem 2011;80:161–87.
[87] Sarvas M, Harwood CR, Bron S, van Dijl JM. Post-translocational folding of secretory proteins in Gram-positive bacteria. Biochim Biophys Acta 2004;1694:311–27.
[88] Krojer T, Sawa J, Schäfer E, Saibil HR, Ehrmann M, Clausen T. Structural basis for the regulated protease and chaperone function of DegP. Nature 2008;453:885–90.
[89] Heuberger EH, Veenhoff LM, Duurkens RH, Friesen RH, Poolman B. Oligomeric state of membrane transport proteins analyzed with blue native electrophoresis and analytical ultracentrifugation. J Mol Biol 2002;317:591–600.

[90] Cao Y, Jin X, Levin EJ, Huang H, Zong Y, Quick M, et al. Crystal structure of a phosphorylation-coupled saccharide transporter. Nature 2011;473:50–4.
[91] Cochu A, Vadeboncoeur C, Moineau S, Frenette M. Genetic and biochemical characterization of the phosphoenolpyruvate:glucose/mannose phosphotransferase system of *Streptococcus thermophilus*. Appl Environ Microbiol 2003;69:5423–32.
[92] Robillard GT, Broos J. Structure/function studies on the bacterial carbohydrate transporters, enzymes II, of the phosphoenolpyruvate-dependent phosphotransferase system. Biochim Biophys Acta 1999;1422:73–104.
[93] Hu J, Hu K, Williams Jr DC, Komlosh ME, Cai M, Clore GM. Solution NMR structures of productive and non-productive complexes between the A and B domains of the cytoplasmic subunit of the mannose transporter of the *Escherichia coli* phosphotransferase system. J Biol Chem 2008;283:11024–37.
[94] Garrett DS, Seok YJ, Peterkofsky A, Clore GM, Gronenborn AM. Identification by NMR of the binding surface for the histidine-containing phosphocarrier protein HPr on the N-terminal domain of enzyme I of the *Escherichia coli* phosphotransferase system. Biochemistry 1997;36:4393–8.
[95] Schwieters CD, Suh JY, Grishaev A, Ghirlando R, Takayama Y, Clore GM. Solution structure of the 128 kDa enzyme I dimer from *Escherichia coli* and its 146 kDa complex with HPr using residual dipolar couplings and small- and wide-angle X-ray scattering. J Am Chem Soc 2010;132:13026–45.
[96] Braun T, Philippsen A, Wirtz S, Borgnia MJ, Agre P, Kühlbrandt W, et al. The 3.7 A projection map of the glycerol facilitator GlpF: a variant of the aquaporin tetramer. EMBO Rep 2000;1:183–9.
[97] Lamarche MG, Wanner BL, Crépin S, Harel J. The phosphate regulon and bacterial virulence: a regulatory network connecting phosphate homeostasis and pathogenesis. FEMS Microbiol Rev 2008;32:461–73.
[98] Cui J, Davidson AL. ABC solute importers in bacteria. Essays Biochem 2011;50:85–99.
[99] Weber J, Senior AE. ATP synthesis driven by proton transport in F_1F_0-ATP synthase. FEBS Lett 2003;545:61–70.
[100] Capaldi RA, Aggeler R. Mechanism of the F(1)F(0)-type ATP synthase, a biological rotary motor. Trends Biochem Sci 2002;27:154–60.
[101] Vicente M, Rico AI, Martínez-Arteaga R, Mingorance J. Septum enlightenment: assembly of bacterial division proteins. J Bacteriol 2006;188:19–27.
[102] Typas A, Banzhaf M, Gross CA, Vollmer W. From the regulation of peptidoglycan synthesis to bacterial growth and morphology. Nat Rev Microbiol 2011;10:123–36.
[103] Gamba P, Veening JW, Saunders NJ, Hamoen LW, Daniel RA. Two-step assembly dynamics of the *Bacillus subtilis* divisome. J Bacteriol 2009;191:4186–94.
[104] Peregrín-Alvarez JM, Xiong X, Su C, Parkinson J. The modular organization of protein interactions in *Escherichia coli*. PLoS Comput Biol 2009;5:e1000523.
[105] Scheffers DJ. Cell wall growth during elongation and division: one ring to bind them? Mol Microbiol 2007;64:877–80.
[106] Lloyd AJ, Gilbey AM, Blewett AM, De Pascale G, El Zoeiby A, Levesque RC, et al. Characterization of tRNA-dependent peptide bond formation by MurM in the synthesis of *Streptococcus pneumoniae* peptidoglycan. J Biol Chem 2008;283:6402–17.
[107] Mohammadi T, Karczmarek A, Crouvoisier M, Bouhss A, Mengin-Lecreulx D, den Blaauwen T. The essential peptidoglycan glycosyltransferase MurG forms a complex with proteins involved in lateral envelope growth as well as with proteins involved in cell division in *Escherichia coli*. Mol Microbiol 2007;65:1106–21.
[108] Tsui HC, Keen SK, Sham LT, Wayne KJ, Winkler ME. Dynamic distribution of the SecA and SecY translocase subunits and septal localization of the HtrA surface chaperone/protease during *Streptococcus pneumoniae* D39 cell division. MBio 2011;2 [doi:pii: e00202-11].
[109] Bogumil D, Dagan T. Cumulative impact of chaperone-mediated folding on genome evolution. Biochemistry 2012;51:9941–53.
[110] Agashe VR, Guha S, Chang HC, Genevaux P, Hayer-Hartl M, Stemp M, et al. Function of trigger factor and DnaK in multidomain protein folding: increase in yield at the expense of folding speed. Cell 2004;117:199–209.
[111] Luirink J, Yu Z, Wagner S, de Gier JW. Biogenesis of inner membrane proteins in *Escherichia coli*. Biochim Biophys Acta 2012;1817:965–76.
[112] Forsbach-Birk V, Simnacher U, Pfrepper KI, Soutschek E, Kiselev AO, Lampe MF, et al. Identification and evaluation of a combination of chlamydial antigens to support the diagnosis of severe and invasive *Chlamydia trachomatis* infections. Clin Microbiol Infect 2010;16:1237–44.
[113] Katakura Y, Sano R, Hashimoto T, Ninomiya K, Shioya S. Lactic acid bacteria display on the cell surface cytosolic proteins that recognize yeast mannan. Appl Microbiol Biotechnol 2010;86:319–26.
[114] Kesimer M, Kiliç N, Mehrotra R, Thornton DJ, Sheehan JK. Identification of salivary mucin MUC7 binding proteins from *Streptococcus gordonii*. BMC Microbiol 2009;9:163.
[115] Ould-Abeih MB, Petit-Topin I, Zidane N, Baron B, Bedouelle H. Multiple folding states and disorder of ribosomal protein SA, a membrane receptor for laminin, anticarcinogens, and pathogens. Biochemistry 2012;51:4807–21.
[116] Bochkareva E, Seluanov A, Bibi E, Girshovich A. Chaperonin-promoted posttranslational membrane insertion of a multispanning membrane protein lactose permease. J Biol Chem 1996;271:22256–61.
[117] Deaton J, Sun J, Holzenburg A, Struck DK, Berry J, Young R. Functional bacteriorhodopsin is efficiently solubilized and delivered to membranes by the chaperonin GroEL. Proc Natl Acad Sci U S A 2004;101:2281–6.
[118] Deaton J, Savva CG, Sun J, Holzenburg A, Berry J, Young R. Solubilization and delivery by GroEL of megadalton complexes of the lambda holing. Protein Sci 2004;13:1778–86.
[119] Kerner MJ, Naylor DJ, Ishihama Y, Maier T, Chang HC, Stines AP, et al. Proteome-wide analysis of chaperonin-dependent protein folding in *Escherichia coli*. Cell 2005;122:209–20.
[120] Veronese PK, Stafford RP, Lucius AL. The *Escherichia coli* ClpA molecular chaperone self-assembles into tetramers. Biochemistry 2009;48:9221–33.
[121] Ling E, Feldman G, Portnoi M, Dagan R, Overweg K, Mulholland F, et al. Glycolytic enzymes associated with the cell surface of *Streptococcus pneumoniae* are antigenic in humans and elicit protective immune responses in the mouse. Clin Exp Immunol 2004;138:290–8.
[122] Proulx M, Duplain L, Lacoste L, Yaguchi M, Lapointe J. The monomeric glutamyl-tRNA synthetase from *Bacillus subtilis* 168 and its regulatory factor. Their purification, characterization, and the study of their interaction. J Biol Chem 1983;258:753–9.
[123] Li H, Wang BC, Xu WJ, Lin XM, Peng XX. Identification and network of outer membrane proteins regulating streptomysin resistance in *Escherichia coli*. J Proteome Res 2008;7:4040–9.
[124] Yang JN, Wang C, Guo C, Peng XX, Li H. Outer membrane proteome and its regulation networks in response to glucose concentration changes in *Escherichia coli*. Mol Biosyst 2011;7:3087–93.

[125] Zeth K. Dps biomineralizing proteins: multifunctional architects of nature. Biochem J 2012;445:297–311.
[126] Goulter-Thorsen RM, Gentle IR, Gobius KS, Dykes GA. The DNA protection during starvation protein (Dps) influences attachment of *Escherichia coli* to abiotic surfaces. Foodborne Pathog Dis 2011;8:939–41.
[127] Eriksen TA, Kadziola A, Bentsen AK, Harlow KW, Larsen S. Structural basis for the function of *Bacillus subtilis* phosphoribosyl-pyrophosphate synthetase. Nat Struct Biol 2000;7:303–8.
[128] Schubert KR, Switzer RL, Shelton E. Studies of the quaternary structure and the chemical properties of phosphoribosylpyrophosphate synthetase from *Salmonella typhimurium*. J Biol Chem 1975;250:7492–500.
[129] Yip LC, Chang V, Balis ME. Membrane-associated purine metabolizing enzyme activities of human peripheral blood cells. Biochemistry 1982;21:6972–8.
[130] Yip LC, Yeh AK, Balis ME. Subcellular distribution of PRibPP synthetase activity of rat intestinal mucosa. Am J Physiol 1980;239:G266–71.
[131] Alderwick LJ, Lloyd GS, Lloyd AJ, Lovering AL, Eggeling L, Besra GS. Biochemical characterization of the *Mycobacterium tuberculosis* phosphoribosyl-1-pyrophosphate synthetase. Glycobiology 2011;21:410–25.
[132] Green SM, Malik T, Giles IG, Drabble WT. The purB gene of *Escherichia coli* K-12 is located in an operon. Microbiology 1996;142:3219–30.
[133] Paoletti L, Lu YJ, Schujman GE, de Mendoza D, Rock CO. Coupling of fatty acid and phospholipid synthesis in *Bacillus subtilis*. J Bacteriol 2007;189:5816–24.
[134] Kvint K, Nachin L, Diez A, Nyström T. The bacterial universal stress protein: function and regulation. Curr Opin Microbiol 2003;6:140–5.
[135] Bieniossek C, Niederhauser B, Baumann UM. The crystal structure of apo-FtsH reveals domain movements necessary for substrate unfolding and translocation. Proc Natl Acad Sci U S A 2009;106:21579–84.
[136] McLuskey K, Paterson NG, Bland ND, Isaacs NW, Mottram JC. Crystal structure of *Leishmania major* oligopeptidase B gives insight into the enzymatic properties of a trypanosomatid virulence factor. J Biol Chem 2010;285:39249–59.
[137] Izard T. The crystal structures of phosphopantetheine adenylyltransferase with bound substrates reveal the enzyme's catalytic mechanism. J Mol Biol 2002;315:487–95.
[138] Buysschaert G, Verstraete K, Savvides SN, Vergauwen B. Structural and biochemical characterization of an atypical short-chain dehydrogenase/reductase reveals an unusual cofactor preference. FEBS J 2013;280:1358–70.
[139] Lauritsen I, Willemoës M, Jensen KF, Johansson E, Harris P. Structure of the dimeric form of CTP synthase from *Sulfolobus solfataricus*. Acta Crystallogr Sect F Struct Biol Cryst Commun 2011;67:201–8.
[140] Saito J, Yamada M, Watanabe T, Iida M, Kitagawa H, Takahata S, et al. Crystal structure of enoyl–acyl carrier protein reductase (FabK) from *Streptococcus pneumoniae* reveals the binding mode of an inhibitor. Protein Sci 2008;17:691–9.
[141] Pang SS, Duggleby RG, Schowen RL, Guddat LW. The crystal structures of *Klebsiella pneumoniae* acetolactate synthase with enzyme-bound cofactor and with an unusual intermediate. J Biol Chem 2004;279:2242–53.
[142] Li JS, Bi YT, Dong C, Yang JF, Liang WD. Transcriptome analysis of adaptive heat shock response of *Streptococcus thermophilus*. PLoS One 2011;6(10):e25777.
[143] Arioli S, Ragg E, Scaglioni L, Fessas D, Signorelli M, Karp M, et al. Alkalizing reactions streamline cellular metabolism in acidogenic microorganisms. PLoS One 2010;5:e1520.
[144] Kleerebezem M, Hols P, Bernard E, Rolain T, Zhou M, Siezen RJ, et al. The extracellular biology of the lactobacilli. FEMS Microbiol Rev 2010;34(2):199–230.